PRODUCTION OF DUCTILE IRON

AND

STUDY OF ITS IMPORTANT PROPERTIES

BY

SYED SHAH ABDUL MOGNI

A theis submitted to the Department of Metallurgical Engineering, Bangladesh University of Engineering and Technology, Dhaka, in partial fulfilment of the requirements for the degree of Master of Science in Engineering (Metallurgical).

December 1992.

#85987#

DECLARATION

This is to assert that this research work has been carried out by the author under the supervision of Dr. Md. Serajul Islam, Professor, Department of Metallurgical Engineering, BUET, Dhaka, and it has not been submitted elsewhere for the award of any other degree or diploma.
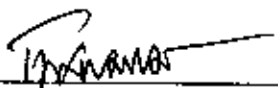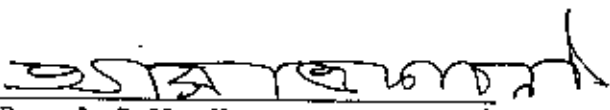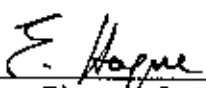
Countersigned:

_____
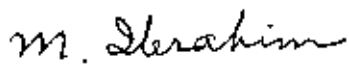Supervisor

_____
Signature of the author

The undersigned examiners appointed by the Committee of Advanced Studies and Research (CASR) hereby recommend to the Department of Metallurgical Engineering of the Bangladesh University of Engineering and Technology, Dhaka, the acceptance of the thesis entitled "PRODUCTION OF DUCTILE IRON AND STUDY OF ITS IMPORTANT PROPERTIES" subimtted by SYED SHAH ABDUL MOGNI, B.Sc.Engg. (Metallurgical), in partial fulfilment of the requirements for the Degree of Master of Science in Engineering (Metallurgical).

1. _____

Dr. Md. Serajul Islam   Chairman
Professor   (Supervisor)
Department of Metallurgical Engineering
BUET, DHAKA.

2. _____

Dr. A.S.W. Kurny
Professor and Head   Member
Department of Metallurgical Engineering
BUET, Dhaka.

3. _____

Dr. Ehsakul Haque
Professor   Member
Department of Metallurgical Engineering
BUET, Dhaka.

4. _____

Professor Dr. M. Ibrahim   Member
House No. 31, Road No. 4   (External)
Dhanmondi Residential Area,
Dhaka.

ACKNOWLEDGEMENTS

The author is deeply indebted to and express his profound gratitude to Dr. Md. Serajul Islam, Professor, Dept. of Metallurgical Engineering, BUET, for his valuable Suggestions, inspiring guidance and constant encouragement in all stages of the project as well as in preparing this thesis.

The author is very much grateful and express his profound gratitude to his ex-supervisor Dr. Md. Mohar Ali, Prof., Dept. of Metallurgical Engineering, BUET, who is now engaged in the post-doctorate programme in the University of Shefield, England, for his kind help at initial stage of this research work. The author is very much indebted to Dr. Mohafizul Haque, professor, Dept. of Metallurgical Engineering, BUET, for the helpful discussions he had with him.

Thanks are also due to Mr. Mollah Ahmed Ali, Superintendent and Chief Instructor, Machine Shop for his kind help in preparing tensile and charpy specimens. Appreciation also goes to Mr. Fazlul Haque Bhuiyan, Senior Foundry Instructor, Md. Lutfor Rahman, Senior Crafts Instructor, Babu Binoy Bhushan Shaha, Senior Laboratory Instructors and other staff members in the Department for their kind help in different stages of this project.

BUET, Dhaka.   THE AUTHOR

ABSTRACT

An attempt has been made to produce ductile iron or spheroidal graphite (S.G) iron and to study its important properties with a view to reducing the import of machinery parts made of S.G. iron.

Locally available (imported) pig iron and locally produced mild steel rods were used to produce S.G. iron in an induction furnace. Calcium carbide was used to reduce the sulphur content of the charge through a prior desulphurization process carried out in the department.

The nodule count, the nodularity and the mechanical properties were found lower in the S.G. iron produced in the first heat when the inoculation treatment was carried out inside the ladle along with spheroidization treatment simultaneously and charcoal dust was used as carburizing material. But these were found better in the second heat when the spheroidization treatment was carried out at first and the inoculation later and graphite powder was used as carburizing material instead of charcoal.

Circular bars having diameter of $\frac{1}{2}$", $\frac{3}{4}$", 1", 1$\frac{1}{2}$", 2" and 2$\frac{1}{2}$"with a height of 3" each were cast with the S.G. iron produced in the first heat to observe the effects of cooling rate on the morphology of graphite, the nodule count, the nodularity and the matrix microstructure. The percentage of cementite was found to increase in the matrix of thinner section bars resulting less number of nodules. Pin like little spheroids were found to increase in number as the diameter of the bars increased. Larger size and lower nodularity of the spheroidal graphite particles were found in thicker bars. Ferrite rings were found in the microstructure of thicker section bars around the spheroidal graphite particles.

Specimens cut from these circular bars were annealed at 950°C for one hour to observe the effect of the annealing treatment on the nodule count, the nodularity and the matrix microstructure. After annealing treatment the number of nodules in thinner section bars were increased many times and the cementite and pearlite matrix of thinner section bars were transformed into fully ferritic matrix. But the matrix of thicker section bars were partially transformed into ferritic matrix.

A few keel blocks were cast with the S.G. iron produced in the first and the second heat to examine the mechanical properties of the S.G. iron along with their metallographic data. It was observed that in the as-cast condition the mechanical properties of the keel blocks produced in the second heat were superior to those produced in the first heat. In the annealed condition the ultimate tensile strength of the specimens from the keel blocks in the second heat was observed to be lower than those in the as-cast condition. It was found that the pouring temperature affected the mechanical properties of the S.G. iron.

CONTENTS

CHAPTER-1

INTRODUCTION

Ductile iron known as nodular cast iron, spheroidal graphite iron and spherulitic iron in which the graphite is present as tiny balls or spheroids, was first declared as a new engineering material at the annual meeting of the American Foundrymen's Society in 1948. Spheroidal graphite iron has special advantages such as low melting point, good fluidity and castability, excellent machinability and good wear resistance like gray cast iron as well as engineering advantages such as high strength, toughness, ductility, hot workability and hardenability like steel. There are three types of S.G. iron in practice. These are pearlitic, ferritic and pearlitic-ferritic S.G. Iron.

The matrix of S.G. Iron can be controlled by proper selection of the base composition, by suitable foundry practice and by heat treatment.

S.G. iron is an important material for cast iron foundry. Heavy duty machineries, dies, rolls for wear resistance, valve & pump bodies, pinions, gears, crank shafts, cams, guides, track rollers, spare parts of agricultural machineries, paper mills, construction and earth moving machineries, I.C. engines and different types of pipe fittings are manufactured by means of S.G. Iron.

A large amount of spare parts and machineries of S.G. Iron required by Bangladesh for its different industries and organizations are now met through import. It is possible to reduce

the import volume of S.G. Iron products by manufacturing this type of S.G. Iron having special characteristics.

S.G Iron foundry will be a profitable concern in our country. But this type of industry is not still established in our country. Many large and small sized foundries have been set up in our country, but these are not producing S.G. Iron because of lack of technical know how to produce this special type of material.

This project has been undertaken in order to produce S.G. Iron locally and to study its important properties. Once this process is established this will be applied commercially to industries in our country. This will help to reduce the import of machinery parts and thus will save our hard earned foreign exchange.

CHAPTER-2

THE FUNDAMENTAL OF S.G. IRON

2.1 The freezing process

The freezing of S.G. Iron is an eutectic transformation. According to the iron carbon equilibrium phase diagram (Fig.1) the meeting point of the liquidus and solidus lines at 4.30% carbon is called the eutectic. Alloys containing less carbon than eutectic are called hypoeutectic and those containing more carbon are called hypereutectic.

Of all the elements (other than carbon) present in S.G. Iron, silicon has the greatest influence on the carbon content of the eutectic. Its effect of moving the eutectic to lower carbon contents can be accounted for by considering how much carbon the silicon is equivalent to in this regard. This "silicon equivalent" is additive to the actual carbon content, and the sum of the two is called the "carbon equivalent". According to the most accurate measurements, 1% silicon lowers the carbon content of the eutectic by 0.31%. The carbon equivalent is therefore expressed as:

C.E = TC (%) + 0.31 Si (%)

On this basis, therefore, if C.E is less than 4.30 the alloy is hypoeutectic, if it is greater than 4.30, the alloy is hypereutectic. R.R. Kust and C.R. Loper[1] reported that a carbon equivalent (C.E.) of 4.3% to 4.65% and preferably 4.45% to 4.55% (percent carbon + 1/3 %Si) for general usage should be maintained to produce satisfactory S.G. Iron. The specific C.E. selection

°C 1539 A

1500 δ+Liq

B

Liquid

1400 γ+δ

D

1300 Austenite

Liquid + Austenite

Fe₃C+Liq.

1200

C'

1100 E 1130° F

2.0

1000

G 910° Austenite +

Austenite+Cementite +Ledeburite

Cementite +Ledeburite

900 Ferrite Austenite

M +Cementite 723°

P S'

700 P 0.80 Pearlite

Pearlite+Cementite +Ledeburite

Cementite K

0.025

600 Pearlite +Ledeburite

200 +Ferrite +Cementite α+Fe₃C

100

0

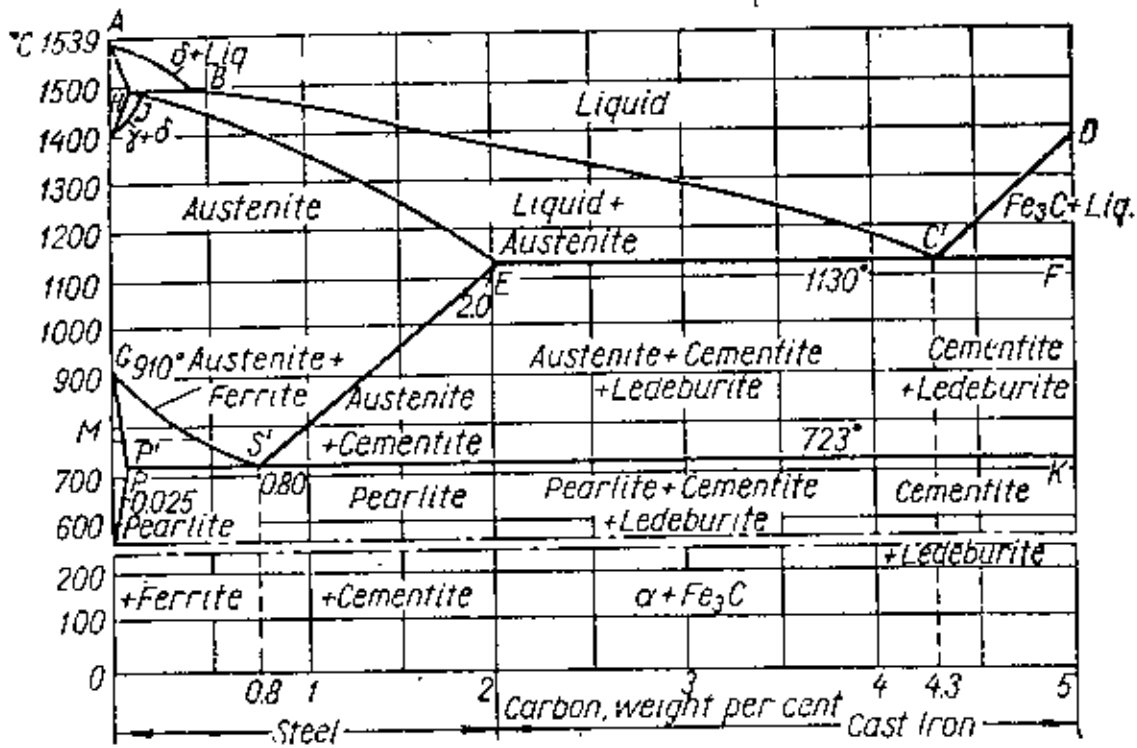0.8 1 2 Carbon, weight per cent 4 4.3 5

Steel Cast Iron

Fig. 1. Iron-carbon equilibrium diagram

will have to be a function of the casting section size, the efficiency of treatment and inoculation, the handling process in use, the specific temperatures involved and finally an analysis of the entire processing operation. For the production of heavy section S.G. Iron castings a balance is usually obtained between C.E. low enough to prevent floatation yet high enough to yield sufficient nodularity within the structure.

It happens very seldom that the carbon equivalent is exactly 4.30 i.e exactly eutectic. Even then, some slight undercooling is unavoidable and this causes both eutectic and slight hypereutectic alloys to start their freezing as if they were hypoeutectic. In the practical sense, then, the freezing mechanism is never eutectic but either hypo or hypereutectic.

2.11 Hypoeutectic freezing

Hypoeutectic S.G. Irons start their freezing with the precipitation of solid iron in the form of branched crystals called dendrites. The process continues with continued heat extraction until the remaining liquid reaches, or cools below the eutectic temperature. Doru M. Stefanescu and Dilip K. Bandyopadhyay[2] reported that, austenite dendrites play a significant role in eutectic solidification of S.G. Iron and that it is possible for austenite dendrites to grow partially independent of graphite spheroids.

After undercooling both graphite and solid iron precipitate simultaneously causing recalescence up to the eutectic temperature,

if cooling is slow enough. The freezing of the eutectic is characterized partially by the continued growth of the austenite dendrites and partially by a coupled growth of both austenite and graphite, the first forming a shell around the latter.

The graphite-austenite globules adhere to one another and to the austenite dendrites as well. In a random fashion, individual groups of globules form, the groups being separated by liquid iron. These groups are called eutectic cells.

At an advanced stage of freezing the melt is depleted in carbon and the cell boundary regions will be mostly graphite free.

2.12 Hypereutectic freezing

The solidification of hypereutectic S.G. Irons is similar to the hypoeutectic ones with the exception that the first (primary) phase to precipitate is graphite in the form of spheroids. Once the liquid is cooled to below the eutectic temperature, the simultaneous freezing of both iron and graphite commences somewhat like in the case of hypoeutectic S.G. Irons. Again, the process is, in part, precipitation of graphite free austenite and, in part, precipitation of globules, the centre of which is a graphite spheroid surrounded by its eutectic partner.

The leading phase is graphite. Graphite-austenite globules are formed in a layer like fashion, the layers being perpendicular to the direction of heat extraction. This phenomenon does not occur in hypoeutectic irons because, initially the leading phase is austenite. As a result, globule distribution will be uniform,

dependent only on gradients of carbon concentration in the liquid.

Once a layer of globules has formed, the liquid next to it is depleted in carbon and will form a layer of graphite free austenite. As the process repeats itself, a layer type structure results in which the graphite free phase resembles dendrites.

2.2 The growth of spheroidal graphite from flake graphite.

The solidification of S.G. Iron takes place in a different way than gray cast iron even though basically they have the same chemical composition except for less sulphur and addition of nucleating agent like magnesium. During solidification of S.G. iron spheroidal graphite eutectics are formed instead of flake graphite formation.

Several theories or hypotheses were developed explaining the shape of graphite.

According to theory the graphite shape is determined by its nucleus. It is assumed in this explanation that certain types of foreign particles (presumably compounds of the spheroidizer element), acting as nuclei, cause the graphite to grow at the same rate in every direction i.e forming a sphere.

The theory depending on branching frequency explains that the graphite shape is determined by the branching frequency of growing graphite dendrites. According to this theory the growth of a graphite spheroid begins like that of a graphite flake. This theory claims that the flake grows in a dendritic fashion. If the branching frequency is low, the formation of graphite flake

results. If the branching frequency is very high due to the presence of spheroidizer, the branches overlap one another with a resultant spheroidal graphite shape.

Another explanation is very similar to the theory of branching frequency with the exception that the growth is eccentric. Because of this eccentric growth, a cabbage leaf type growth of graphite occurs. Aa a result of this type of growth flake graphite are transformed into the spheroidal graphite shapes.

In respect of surface energy another hypothesis explains that spheroidal graphite represents minimum surface energy. Keverian and taylor[3] state that a high graphite-melt interfacial energy favours graphite spherulite formation. In ordinary cast iron flake like shapes are the first graphite elements to form by growth in the closed packed direction or "a" direction. In the preaence of impurities (sulphur is the most important element in this respect) this growth form is stabilized and the flake-shape persists. Sulphur lowers the graphite/melt interfacial energy on the prism compared to the basal planes. In the presence of such elements as Magnesium (others are Te, B, Pb, Bi and Ce) or super pure melts of Fe-C-Si, graphite/melt interface while still growing in the a-direction bend and curve so that growth takes place in a circumferential direction rather than a radial one and with the basal plane being the major crystallographic plane in contact with the melt. The bending of graphite to form a spheroid is a result of twinning and the formation of low energy grain boundaries. It has been suggested that spheroid shape could be a result of

multiple cone-helices a cone being generated by crystallographic rotation.

Still another theory explains that the spheroidal shape is the result of graphite growth within solid iron. According to this theory, the graphite flakes grow in the direct contact with the liquid. Because of the effect of spherodizing treatment, the growing graphite crystals are completely surrounded by solid iron (austenite). As the growth rate is therefore controlled by the rate of diffusion of carbon, it will be approximately uniform in all directions and thus a spheroid forms. C.R. Loper and R.W. Heine[4] reported that spheroidal graphite is allowed to nucleate at high temperatures by the magnesium inoculation. The graphite spheroids are then protected by an austenite shell as the liquid cools. The growth of the spheroids to larger sizes occurs during the eutectic arrest temperature similar to the eutectic arrest observed in gray iron.

C.R. Kellerman and C.R. Loper[5] reported that the spheroidal shapes were observed to be nucleated at temperatures considerably above the flake graphite eutectic start temperature and developed an apparent protective austenite shell above the eutectic-start temperature. Growth of the spheroids then occured within the austenite shell which separated all of the spheroidal graphite shapes from the liquid. This austenite shell served to protect the graphite from the liquid during cooling through the flake graphite nucleation and growth temperature range.

2.3 Solid State Transformation

The structure of S.G. Irons consists of graphite spheroids embedded into what is called the matrix. The amount of graphite is about 8 to 10 volume percent. Carbides (Fe_3C) may also be present but this, with the exception of most types of austenitic S.G. Irons, is undesirable. Carbides drastically reduce both strength and toughness.

Upon completion of freezing, the matrix of unalloyed or moderately alloyed S.G. Irons is homogeneous austenite, containing approximately 1% carbon in solid solution. As S.G. Iron Cools, the solubility of carbon in austenite decreases. The rejected carbon migrates to and deposits itself onto a graphite spheroid. This process may continue down to room temperature only if the S.G. Iron is heavily alloyed with nickel (18% Ni minimum).

In unalloyed grades austenite is not stable to room temperature and must transform into another crystallographic variety of iron: ferrite. The temperature of this transformation is influenced by silicon content but cannot be lower than 1300^0F (723^0C).

The austenite-ferrite transformation in S.G. irons also entails a change in the carbon content of the matrix.

The carbon content of the austenite is about 1% at the temperature of its crystallization and decreases upon cooling. At the temperature of the austenite-ferrite transformation the solubility of carbon in austenite is about 0.55% (Si:2.5%). In contrast, for all practical purposes, no carbon can be dissolved in

ferrite. Carbon is, then, rejected during transformation. Just what happens to the carbon depends on chemical composition, cooling rate, and graphite distribution. Under favourable conditions and when the rate of cooling is slow, all carbon will migrate to and become part of the graphite spheroids.

Fast cooling and other influences do not permit the migration of carbon. This does not alter the fact that carbon is insoluble in ferrite and that austenite must transform. The way out of this fact is that very thin platelets interrupt the continuity of and alternate with those of ferrite. The resulting matrix structure is called pearlite.

The as-cast matrix structure of S.G. irons most often contain both ferrite and pearlite in various proportions. Ferrites are found to surround the graphite spheroids.

There are three more matrix components possible in S.G. irons. If cooling from the temperature of homogeneous austenite extremely fast, (quenching in oil or water) austenite is still required to transform but practically no time is left for carbon migration. The atoms of carbon remain in situ and distort the crystal lattice of ferrite to such a degree that a modified, diamond-type crystal lattice forms.

In producing a martensitic matrix, carbon is forced to stay in place. The structure is stable at or below room temperature. When, however, the casting is heated to a temperature between 800 and 1300^0F, martensite transforms into a ferrite base, the rejected carbon forming very small globules of carbide. The higher the

temperature of the "tempering" treatment the coarser and softer the matrix.

2.4 Elements influencing the distribution and shape of graphite.

Graphite distribution is defined as the number of graphite spheroids per unit of volume. Its value is directly proportional to, and most conveniently measured by, the number of sections of graphite spheroids per unit of surface area on a straight plane across the sample. Most commonly the number of spheroids per square millimeter is reported.

The one element which influences the distribution of graphite spheroids in a semichemical way is silicon. The higher the Si-content, the higher the nodule count. Many other elements affect nodule count through their influence on nucleation.

With respect to their influence on graphite shape, chemical elements have been categorized in the past into three groups: a) beneficial b) neutral and c) deleterious. A few examples of each are listed below:

Beneficial	Neutral	Deleterious
Mg, Ce, Ca, and	Fe, Si, Ni,	Al, Sb, As, Bi, Pb. Ti
all other spheroidizers	Mo, C	

Carbon content influences both graphite size and shape, particularly through its influence on carbon equivalent. Graphite spheroids are smaller and better shaped in hypereutectic SG irons.

The effect of silicon can be either beneficial or harmful. On the one side, increasing Si content increases nodule count and generally improves spheroid shape. On the otherside, increasing silicon content is known to promote chunk-type graphite deterioration in heavy S.G. iron castings.

The combination of high nickel and silicon contents leads to chunk-type graphite deterioration. This effect is commonly observed in high nickel alloyed (austenitic) S.G. irons of medium to heavy section thickness.

Elements (e.g. As, Sb) traditionally considered as harmful even in minute concentrations are now being deliberately added in laboratory and in limited commercial practice in order to improve spheroidal graphite shape or sometimes to promote pearlite. In both cases cerium is also added.

Alloys with a fully spheroidal graphite structure have been obtained as a result of the addition of one or more spheroidizing elements, the group of which consists of Mg, Ce, Ca, Li, Na, K, Sc, Be, Y and some others. These elements are properly considered as graphite shape active. Other elements known to be graphite shape active are: Al, As, Bi, C, Cd, Cu, Ni, Pb, Sb, Se, Si, Sn, Te, Ti, Zn, Zr and all or many of the rare earths.

Graphite in S.G. iron is spheroidal rather than spherical. Common objectionable deviations from spheroidal shape are flake graphite, chunk graphite, compact graphite, vermicular graphite and exploded graphite.

Compact graphite refers to graphite shapes which deviated from

being spheroidal by their ragged and irregular shape. Vermicular graphite refers to shapes varying from short, stubby graphite to more worm like graphite shapes.

Elements which cause intercellular flakes are apparently rejected from the growing solid cell, segregate into the last liquid to freeze and, in this liquid, may reach a concentration sufficient to cause flake graphite to precipitate. As a consequence, intercellular flake graphite is more commonly encountered in heavy S.G. iron castings, where ample time is available for segregation. N.L. Charch and R.D. Schelleng [6] reported that calcium can cause the formation of vermicular graphite near the thermal center of heavy S.G. iron castings. R.K. Buhr [7] stated that the addition of a small amount of Pb to the normal charge was found to beneficial in reducing vermicular graphite formation in heavy sections.

Chunk graphite forms within the cells, while the cell boundaries may, and usually do, contain some well formed spheroids. The effect of some flake promoting elements can be neutralized by the addition of some element which promotes chunk graphite. Conversely, chunk graphite can be eliminated and fully spheroidal graphite structure restored through the addition of some element(s) which promote intercellular flakes. Elements known to oppose each other in this "War" between flake and chunk graphite promotion are:

Elements known to promote chunk graphite	Elements known to promote intercellular flake graphite
Ce, Ca, Si, Ni	Bi, Pb, Sb, As, Cd, Al, Sn, Cu.

Chunk graphite has been eliminated in heavy S.G. iron castings through the addition of 0.002% of any one of four elements: Pb, Sb, As, Bi. The flake graphite promoting effect of 1% aluminium has been successfully neutralized by the addition of 0.03% Ce.

Exploded graphite most commonly occurs in the flotation zone of strongly hypoeutectic S.G. irons. C.R. Loper and R.W. Heine[8] reported that carbon equivalent should be held below about 4.60% to avoid exploded graphite and flotation.

The best graphite shape active element to mention is sulphur.

2.5 Matrix control through chemical composition (unalloyed and moderately alloyed).

The properties of S.G. irons are determined by their matrix structure.

Of the common elements present in S.G. irons, carbon exerts no effect on matrix structure. Silicon, on the otherhand is very influential on pearlite/ferrite ratio, the hardness of ferrite, impact test energy, impact transition temperature and thermal conductivity.

The contents of manganese should never be chosen with the aim of controlling matrix structure. The only single aim in selecting manganese content is freedom from carbides as-cast.

According to some claims, however, the tendency to form

ferrite is influenced by Mn/S ratio. At about a 2.6% Si-content, maximum ferrite content is claimed to be obtainable when Mn content is about 15-17 times that of S-content.

Moderate alloying is done for promoting pearlite. It is stated[9] that manganese must not be used for pearlite promotion. Research in France lists eight elements which promote pearlite with factors of potency assigned. These are (in decreasing order):

Element	Relative pearlite promoting effectiveness
Sn	39.00
Mo	7.90
P	5.60
Cu	4.90
Ti	4.40
Mn	0.44
Ni or Cr	0.37

Pearlite promotion with manganese was also found inferior to that by copper in a Belgium study. Research reported in the U.S.A.[9] compared pearlite promotion by Cu and Sn. The following Cu/Sn combinations resulted in 99% pearlite content:

Cu%	Sn%
1.5	0
1.0	0.03
0.5	0.07
0.25	0.15
0	0.24

Bainitic matrix may be obtained either as-cast or via isothermal heat treatment. In either case, S.G. irons are to be alloyed with a combination of Mo and Ni.

2.6 Desulphurization

Iron should be desulphurized prior to spherodizing treatment for the sake of both economy and cleanliness. Sulphur content in base iron should be held as low as possible for best efficiency in the nodularizing treatment. Nodularizing agents such as Mg and rare earths, react first with sulphur in the iron and until substantially all the sulphur is combined the nodularizing action cannot take place. S.G. iron can be produced more easily and economically, if the sulphur content of the base iron is lowered.

A variety of compounds are used to remove sulphur from molten iron. More practical desulphurizing agents are as follows:

Caustic Soda (NaOH), soda ash (Na_2CO_3), Burnt lime (CaO), lime stone ($CaCO_3$), calcium Carbide (CaC_2) and calcium cyanamide ($CaCN_2$).

Of these, caustic soda is rarely used because of the health hazard it presents, limestone is first reduced to Cao before it desulphurizes and ($CaCN_2$) should be ruled out because it increases base iron nitrogen content with the resultant danger of nitrogen gas defects in the castings.

In the tradition of ferrous metallurgy, CaO is the most established of the desulphurizing compounds. In S.G. iron practice it is used in basic cupola and basic electric arc melting. On rare occasions ($CaCO_3$), (limestone) is injected into large ladles resulting in both economical and excellent desulphurization. According to one report[9], the injection of 0.5% ($CaCO_3$) at a rate of 30-35 lbs/min reduced the S-content of 60 tons of molten iron from 0.06 to 0.008%. The method is limited to large quantities of

iron because of the large temperature loss.

CaC_2 is the another important desulphurizer, which is being used most commonly in desulphurizing practice. The injection of calcium carbide into the base iron used for producing S.G. iron has three definite advantages: The first is a reduction in magnesium and cerium content due to removal of sulphur and promotion of the formation of spheroidal graphite with a lower residual magnesium. The second advantage is that the calcium carbide treatment reduces the tendency to form cementite in the as-cast spheroidal iron. The third benefit of carbide treatment is better control of the final product due to a minimum of variation in base sulphur analysis and residual magnesium.

For the case of CaC_2, research in Canada has developed[9] an accurate formula for the evaluation of desulphurizing efficiency:

$$E = \frac{\log S_0/S_f}{\% \ CaC_2}$$

Where S_0 and S_f are initial and final sulphur contents (%); % CaC_2 = quantity of CaC_2 added in weight percent.

The advantage of this formula is that the efficiency values (E) can be compared for different methods or practices and differences will reflect on the efficiency rather than on the rate of S-transfer to CaC_2. The rate of S-transfer is of course dependent on the initial S-content.

It has been observed that the efficiency of desulphurization with the injection method consistently increased with decreasing

CaC_2 particle size. A most interesting finding is that increasing the total surface area of the injected CaC_2 did not increase the rate of sulphur transport. In the given experiments[9] regardless of particle size, about 8 to 10% of the radius of the CaC_2 particles was converted to C_aS. If dwelling time inside the melt had been longer, a much deeper penetration could have been achieved.

Therefore the efficiency of desulphurization is dependent not only on the total CaC_2 surface area presented to the liquid iron but, also, on the rate of sulphur transport to these surfaces. Since the latter is dependent on the S-content of the iron, three basic variables influencing desulphurizing efficiency are:

a) Degree of stirring and dwelling time,

b) Injection rate, and

c) CaC_2 particle size.

As a general rule, 1% CaC_2 or Na_2CO_3 is needed to reduce base iron sulphur content from 0.1 to 0.01%. It can be either more or less depending on desulphurizing efficiency. J.M. Crockett and H.E. Henderson[10] reported that a reduction in the spherodizing alloy addition of 30% is possible when calcium carbide is injected prior to the alloy treatment. They also reported that, calcium carbide treatment reduces the tendency to form cementite in the as-cast structure of spheroidal graphite cast irons.

CaC_2 reacts as a desulphurizer as follows:

$$FeS + CaC_2 + O_2 = CaS + Fe + 2\ CO.$$
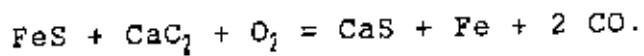
Proper care should be exercised with the spent CaC_2 slag since it invariably contains some active CaC_2. This reacts with water producing acetylene gas and constitutes a fire hazard. The spent slag should be carried outdoors frequently and soaked in water there.

Soda ash is seldom used as desulphurizer because of its harmful environmental effects. It has been observed[11] that desulphurzation of cast iron by the process of electrolysis can attain a higher percentage of desulphurization (upto 97.5%) which can not be reached by any other method.

2.7 Spheroidizing Treatment

Spherodizing treatment is used to transform the flake graphite of the base iron to nodular form in the production of S.G. iron. A number of alloys have been developed for the purpose of spherodizing treatment. The main alloy types are:

1. Magnesium-nickel alloys

    a) 15% Mg., 85% Ni

2. Magnesium-Ferrosilicon alloys:

    a) 9% Mg, 4.5% Si, 1.5% Ca, balance Fe.

    b) 9% Mg, 4.5% Si, 1.5% Ca, 0.5% Ce, balance Fe.

3. Magnesium-silicon alloys:

   a) 18% Mg, 65% Si, 2% Ca, 0.6% Ce, balance Fe.

Although a number of elements are capable of spherodizing the graphite, only magnesium usually together with some calcium, cerium and some other earth elements is commonly used for this purpose. Magnesium is usually alloyed with other elements in order to reduce the volatility of the spherodizing reaction. Gries and Maushake[12] have summarized the work of many other investigators and the following list contains the more popular views of the role of magnesium in S.G. irons: i) the nucleus of spheroidal graphite is a compound of magnesium, ii) magnesium 'poisons' the nucleus for flake graphite, thus causing spheroidal graphite, iii) cerium and magnesium retard or prevent the nucleation of graphite until late in the freezing process, and iv) cerium and magnesium forms sulphides which then promote the formation of spheroidal graphite.

The minimum magnesium content required in the casting to spheroidize the graphite may be as little as 0.01% or more than 0.02%. If magnesium is the only spherodizer added, its concentration must not be less than 0.02%. Additions of cerium, other rare earths and calcium reduce the minimum Mg level down to but not below 0.01%. Less amount of Mg than desired level arises difficulty in S.G. iron as well as large amount of Mg results Mgs inclusions. For this reason, foundries which treat relatively high sulphur containing base irons often specify high minimum magnesium contents upto 0.05%. There exists numerous formula for the calculation of the quantity of magnesium to be added. Of all these the simplest and safest is presented below:

$$\text{Mg to add.(\%)} = \frac{\text{Mg content desired (\%)} + \text{Base S (\%)}}{\text{Mg recover (\%)} \times 0.01}$$

Excessive Mg-contents are detrimental by causing carbides as-cast and increasing shrinking tendency. Control to between a ± 0.015% range of the retained Mg-content is feasible with most treating methods. The most commonly used particle size range for MgFeSi alloys is 2 inch (50mm) maximum and 1/8th inch (3 mm) minimum.

The fading of the spherodizing effect is a very complicated phenomenon. Its simplest component is less of magnesium content through oxidation or combining with sulphur. The reaction is as follows:

$$Mg + O = Mgo$$
$$Mg + S = Mgs$$
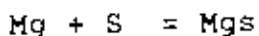
Considering the relative stabilities of the above two compounds, a more likely reaction is as follows:

$$Mg + SiO = Mgo + S.$$
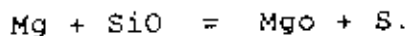
If the source of oxygen is an oxide, silica, as an example, the corresponding reactions are:

$$2 \, Mg + SiO_2 = Si + 2 \, Mgo, \text{ and}$$
$$2 \, Mgs + SiO_2 = Si + 2 \, Mgo + 2S.$$
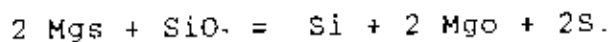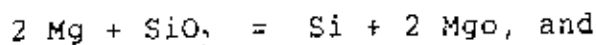
The fading rate is influenced by the following factors:

a)   Initial Mg-content, the higher the faster the fading.

b)   Temperature, the higher the faster the fading.

c)   Slag handling, the faster the slag is removed, the better.

d)   Furnace lining, the worst is silica, the best is magnesia.

Additional fading is manifested in decreasing nodule count and deterioration of graphite shape.

There are sixteen different methods of spheroidizing treatment. But the largest volume of S.G. iron is being produced with the ladle transfer method, because of its simplicity. In this method the magnesium master alloy is placed on the bottom of the empty treatment ladle and liquid base iron is poured over it. It is believed that the stream of the liquid iron must be directed away from the location of the alloy and also, ladle filling must be very fast.

A popular variation is the sandwich method in which the master alloy is covered with small pieces of steel sheet. Such a cover is used to delay the onset of the reaction (the vaporization and burning of the spherodizer element) and to lower locally the temperature of the liquid around the master alloy. While treating with the ladle transfer method, damping the liquid iron over the treatment alloy should be as fast as possible. The ladle transfer treatment with magnesium based master alloys is a relatively violent process. Both for the sake of improving magnesium recovery and for preventing iron from spilling out of the ladle, the ladle

90 cm

60 cm

24 cm

34 cm

ø 24 cm

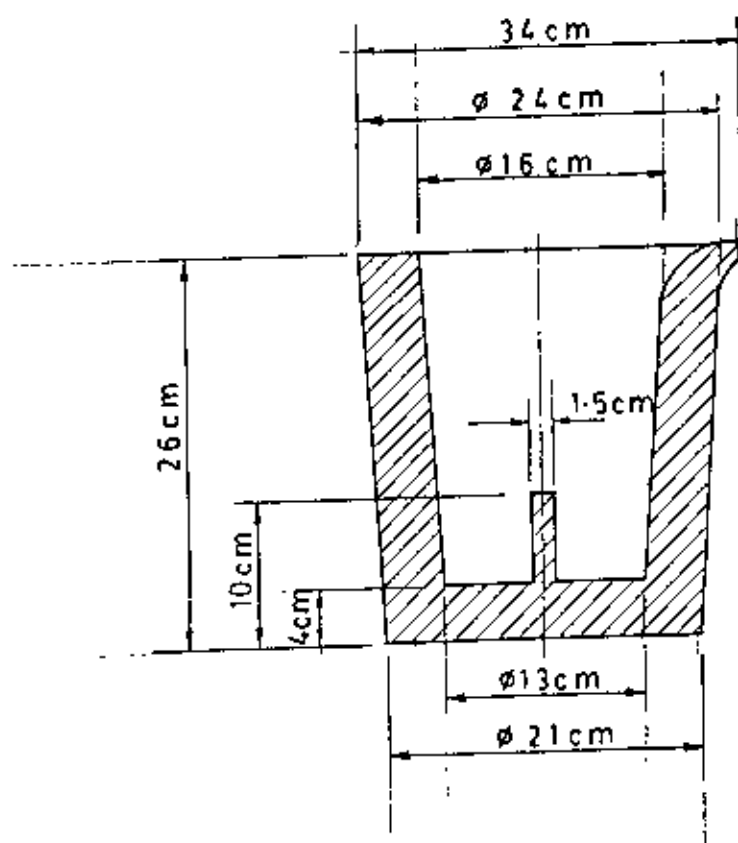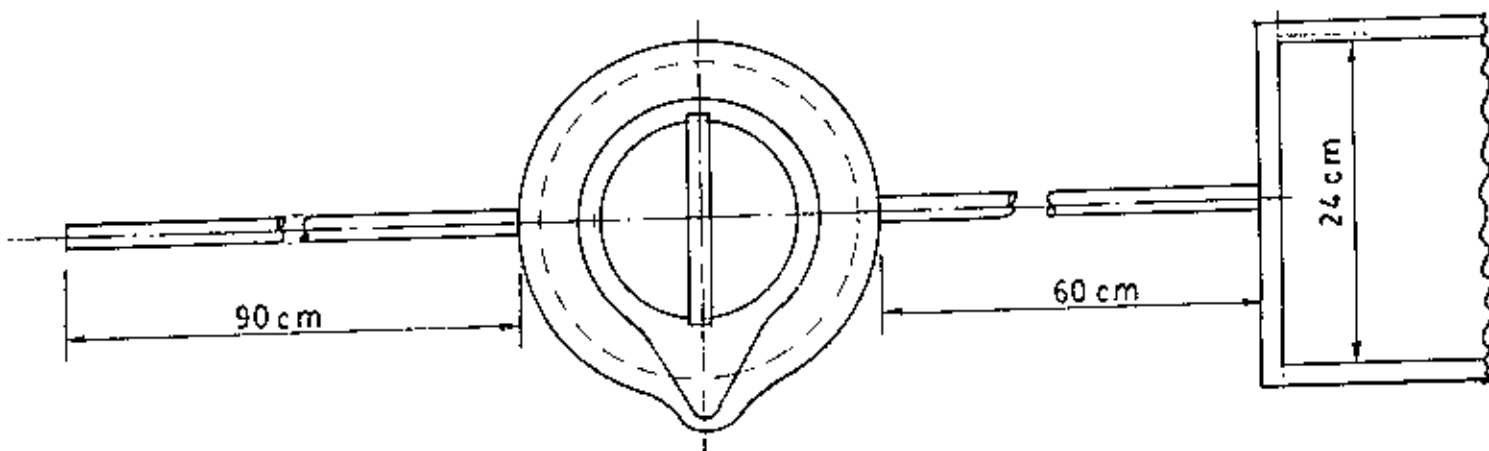ø 16 cm

1·5 cm

26 cm

10 cm

4 cm

ø 13 cm

ø 21 cm

Fig. 2 Covered ladle for Magnesium Treatment

should be relatively tall as shown in fig 2. For the same reason, the treatment ladle should not be filled to more than 2/3 of its holding capacity. The height of the ladle should be twice as high as the diameter of the ladle.

When the treatment ladle is covered with a lid as shown in fig-2, the rate of filling is limited, magnesium recovery is improved substantially, and the reaction violence and Mgo dust formation are minimized. E.V. Kovalevich et al[13] stated a new technology in S.G. iron production named as MDS process in which magnesium recovery is raised efficiently.

2.8 Inoculation

Although the magnesium treatment is responsible for the development of spheroidal graphite, quality S.G. iron also requires the use of an inoculant. Inoculation or post inoculation, refers to the practice of making an addition to the melt which will increase the number of spheroids formed during solidification. The inoculation of S.G. irons produces heterogenious nuclei for the graphite spheroids. When treated with the spheriodizer, S.G. iron is in a semi-inoculated condition to a larger or lesser degree. A separate inoculation improves structures by increasing nodule count and preventing carbides from forming.

The inoculation is dependent on a) the melt, and b) the quality and quantity of the inoculant added. Superheating of melt also influences the inoculation. The effect of the ratio between silicon content of the untreated base S.G. iron and silicon added

with the inoculant exerts a considerable effect on the structure. If this ratio is infinitely large i.e. the iron is not inoculated at all, the metallurgical quality is poor. Similarly if the same ratio is zero, i.e. no silicon is present in base iron, poor quality results. Optimum quality is obtained between the two extremes.

Ca, Al, Ba, Sr, etc. are example of active inoculating elements. For effective and well controlled inoculation, ferro-silicon of controlled chemical compositions are utilized. These alloys are produced in a variety of grades, the most common, however, are the 50, 65, 75, 85 and 90% Si grades. All these grades can also be obtained with or without calcium addition. New and significant entries into the inoculant market are those containing a small amount (1-2%) of magnesium. All inoculants contain relatively little aluminium because aluminium promotes subsurface hydrogen pinhole defects, particularly in thin sections.

The sizing of the inoculant is usually half inch (13 mm) maximum. Since fine particles do not inoculate effectively, a minimum size limit of 1/6 inch (15 mm) is advisable.

The traditional and still most common method of inoculation is to add the inoculant into the stream as the pouring ladle is being filled from the treatment ladle. It has now been found (14) that S.G. iron castings can be produced efficiently and consistently using a process in which a magnesium containing agent i.e. spherodizer and silicon containing treatment agent i.e. inoculant is added to a stream of molten iron in the sprue of a mould if the

mould contains a ceramic filter and the parts of the mould have a defined relationship one with another and if the particle size of the treatment agent is controlled.

It is found in Canadian research[9] that the effectiveness of inoculation sharply decrease with increasing inoculating temperature (Fig. 3). For this reason post inoculation is more effective because it is done at a temperature lowered by the cooling effect of the treatment. C.L. toggle and R. Carlson[15] found in their industry that the optimum nucleation for carbide elimination from minimum additions of ferrosilicon was dependent on the following factors:

a. Mechanics of inoculation,

b. Carbon equivalent of S.G. iron,

c. Melting methods - cupola vs. electric arc,

d. Magnesium level of S.G. iron,

e. Sizing of inoculants,

f. Calcium and aluminium content of inoculants,

g. Aging of inoculants with reservation as to the degree,

h. Forms of Ca present,

i. Other elements alloyed with FeSi-strontium and

j. Solidification patterns.

Trojan, P.K. Bargeron, W.N. and Flinn. R.A.[16] reported that increased post inoculation amount in hypereutectic irons does not affect percentage nodularity, has little effect on module count, decreases ultimate tensile strength, while increasing elongation (ferritizing effect) and reduces carbide formation in this
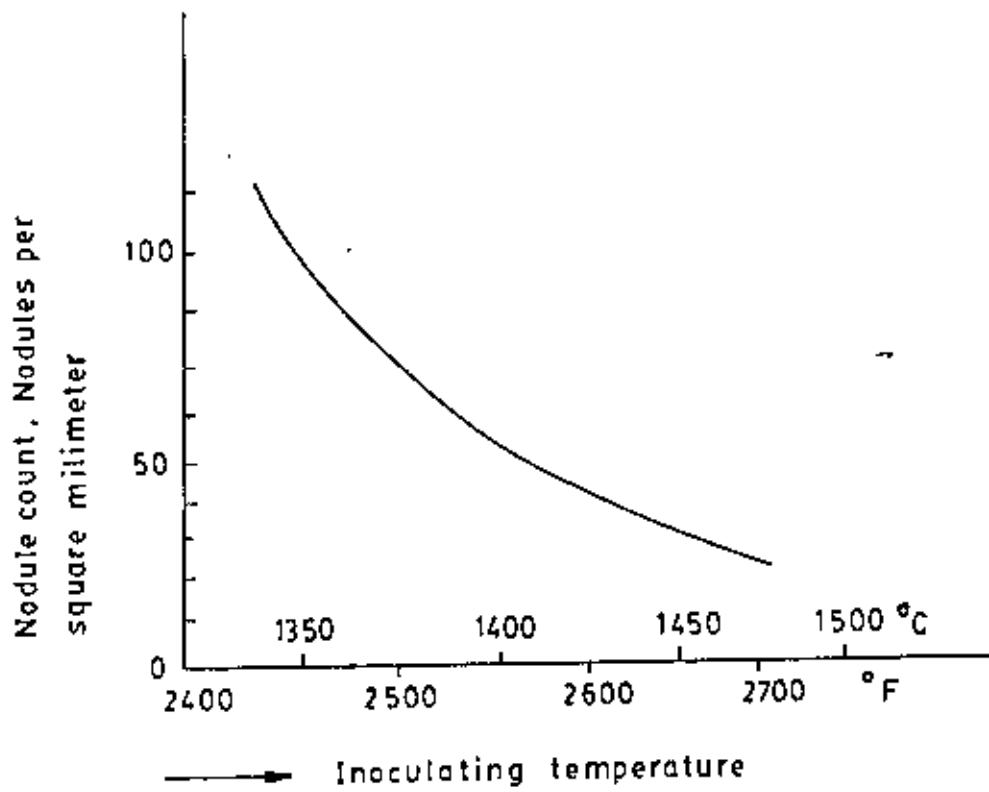
Fig. 3 The effect of temperature on the inoculated condition

sections. On the otherhand Dawson, J.V.[17] reported that increased amount of post inoculant in hypoeutectic irons produce higher nodule counts. W.F. saw and T. Watmough[18] stated that 0.55% Si addition as the post inoculant will be optimum when high nodule counts, good nodule distribution and nodule sizes are considered. W.J. Dell and R. J. Christ[19] investigated and reported that mold inoculation is more effective than the usual ladle addition method. They reported that post inoculation directly into the mold with as little as one gram of calcium bearing regular grade 85% ferrosilicon drastically reduces both general and inverse chill in S.G. iron.

R.R. Kust and C.R. Loper stated[1] that S.G. iron structures are considerably improved if a practice of post inoculation with ferrosilicon is followed after magnesium treatment has taken place. Mold inclulation also increases the number of nodules in the structure. W.J. Dell and R.J. Christ[19] reported that direct mold inoculation could produce numerous tiny concentration cells of graphitizers promoting graphite nucleation.

Carbide free microstructure in this sections is possible with ferrosilicon post inoculation of the metal stream between the casting machine ladle and the mould. Direct mould inoculation can produce numerous tiny concentration cells of graphitizers promoting graphite nucleation. Immediate solidification of the iron in the mould prevents self homogenization that destroys these concentration cells. For this reason, inoculation directly into the mould should yield maximum effectiveness in eliminating carbides.

2.9 Heat treatment of S.G. iron

The heat treatment of S.G. iron is practiced in order to a) increase dimensional stability, b) decompose as cast carbides and cause a predetermined matrix structure, c) alter matrix structure, d) harden some or all external surfaces and e) minimize temper embrittlement.

But standard heat treatment may fail to decompose all the as-cast carbides or provide for an all ferritic annealed structure unless chemical composition and other production variables are under control.

These five types of operation are explained as follows :

a) Heat treatment to increase dimensional stability

This stress relieving treatment is exercised when high dimensional accuracy is required, particularly at elevated temperatures.

Depending upon size and shape all castings have some locked in stresses. In the case of gray irons, some of the stress will be eliminated at room temperature via plastic deformation, which is a lengthy process, and equilibrium will only be reached after one year or more. In contrast, part of the stress in S.G. irons is relieved automatically via elastic deformation which is an instantaneous process. Still, after equilibrium is reached, some stresses remain.

Some, but very little stress may be relieved by applying external stresses (vibration). If maximum freedom from internal
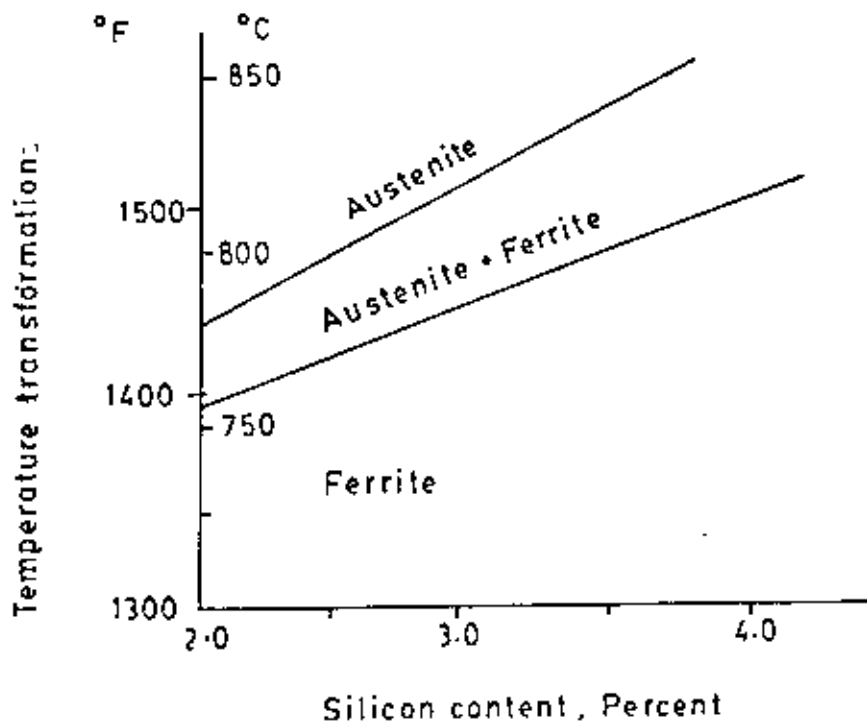
Fig. 4 Ferrite-Austenite (critical) transformation temperature range as a function of silicon content

stresses is necessary, the casting must be treated at a temperature where plastic deformation occurs at a relatively high speed.

In order not to alter the matrix, this temperature is normally selected to be $1100^0F(595^0C)$. A five-hour hold at this temperature is recommended. Still longer holding times remove relatively little extra stress. The subsequent cooling should not exceed a rate of 100^0F/hour $(55^0C/H)$. After this the castings are air cooled.

b. Softening Heat treatment

The purpose of all softening heat treatments is to :

i) decompose as-cast carbides (if present), and ii) produce a ferritic matrix.

i) Full annealing:

The first part, the decomposition of Carbides, takes place at a temperature of 1650^0C (900^0C) with a holding time of two hours. Longer holding times for thick castings are needed only for temperature-homogenization. The rule is one extra hour holding for every 1 inch (25 mm) thickness above 1 inch (25 mm).

The casting is now cooled to about 100^0F (55^0C) below the lower critical temperature (Fig. 4) and held there for 5 hours plus 1 hour for every 1 in (25 mm) thickness.

S.G. irons which are low in pearlite stabilizing elements such as copper or manganese, may be ferritized without the lengthy holding. Instead, the casting is cooled slowly through and below the critical transformation range (Fig. 4). Maximum cooling rate

with 0.1% Mn-content is 100^0F/hour (55^0C/hour) and with 0.5% Mn-content, 35^0F/hour (20^0C/hour). Slow cooling should continue to 1100^0F (595^0C) after which the casting may be air cooled.

ii) Sub-critical annealing

If the castings are known to be carbide-free, ferritizing may be achieved through heating to 100^0F (55^0C) below the lower critical temperature, holding for 5 hours plus 1 hour per 1 inch (25 mm) thickness, cooling slowly to 1100^0F (595^0C) and air cooling.

C. Strengthening heat treatment

i) Normalizing

Depending on the presence or absence of as-cast carbides, austenitizing should be done either at 1650^0F (900^0C) (Carbides present) or about 50^0F (28^0C) above the upper critical temperature (Carbides absent). Holding time is 1 hour plus one additional hour per 1 inch (25 mm) wall thickness.

Cooling from the above temperature may be in still air, forced air (above 1-½ in (38 mm) thickness). Or with water-mist spray above 2-¼ in (63 mm) thickness. Castings more than 1 inch (25 mm) thick are usually alloyed with 0.5-2.0% Cu to aid normalizing. The more copper the thicker the casting.

Due to stresses created by the relatively fast cooling, normalizing is often followed by stress relief (draw).

ii) Double Normalizing

This variety of normalizing was developed in Japan and starts with a high temperature homogenizing at 1700^0F (925^0C). After this, the piece is furnace cooled at 50^0F (28^0C) above the upper critical temperature (Fig. 4). After a short hold the casting is cooled as in conventional normalizing.

In comparison with conventional normalizing:

Yield strength decreases by an average of 2%.

Hardness decreases by an average of 10%.

Elongation increases by an average of 50%.

Impact resistance increases by 50 to 150%.

iii) Quenching - Tempering

This treatment is not recommended partly because of a distinct longer of cracking of the casting during or shortly after quenching and partly because the properties are not significantly superior to those obtainable through normalizing.

Quenching is preceded by austenitizing at 100^0F (55^0C) above the upper critical temperature. After a temperature homogenizing hold (1 hour plus etc.) the casting is quenched to a temperature not exceeding 200^0F (93^0C), usually in an oil bath. The structure is now martensitic. The rate of cooling prior to the austenite-martensite transformation is important. Its required value as well as the temperature of the transformation depends on alloying.

Cooling conditions during quenching permit some carbon diffusion, the carbon may migrate to and become part of a spheroid.
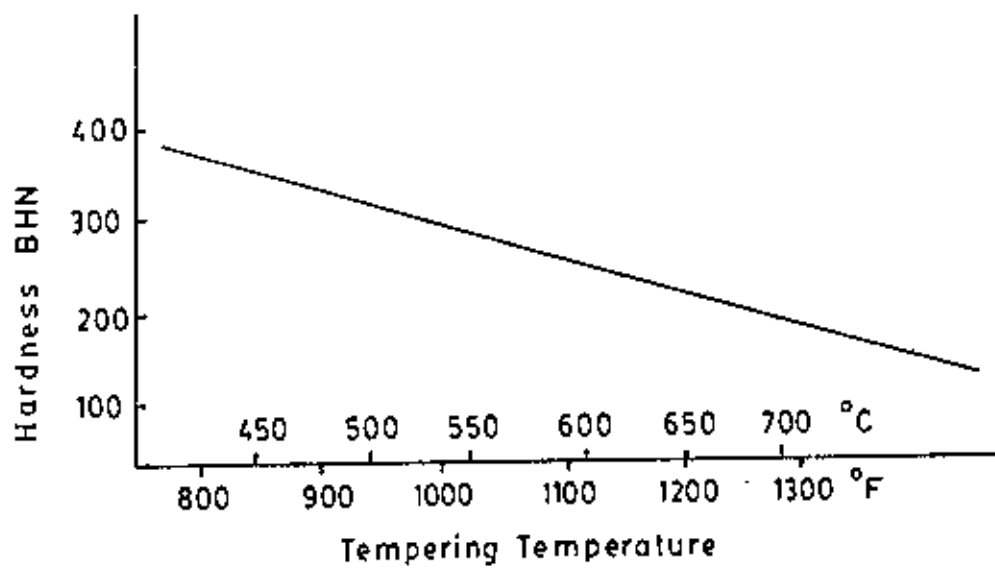
Fig. 5   Hardness Vs Tempering Temperature

Oil quenched 1 inch or thicker S.G. iron pieces are cooled fast enough in order to avoid transformation to pearlite. These may be cooled slowly enough to allow carbon to migrate to the graphite spheroids, depleting the undercooled austenite of carbon and allowing part of the austenite to transform into ferrite. A small quantity of ferrite may form in this way.

Quenching may be followed by deep freezing in dry ice or liquid nitrogen. This provides for a fully martensitic structure, transforming the remaining austenite. Since, however martensitic S.G. irons find practically no application, deep freezing is seldom performed.

Quenching is normally followed by tempering at a pre-determined temperature (for one hour etc.). Resultant hardness depends on temperature and is highly predictable. The temperature hardness relationship is shown in Fig. 5.

iv) Martempering

This treatment applied to steels, can also be used to render the structure of a S.G. iron casting martensitic through its section.

The quenching which follows proper austenization is interrupted somewhat above the MS temperature and the casting is held isothermally until differences between outside and interior are practically eliminated. The piece is then rendered martensitic throughout by simple air cooling. Tempering follows this treatment with rare exception.

v)   Austempering

The purpose of austempering is to render the matrix bainitic (accicular). Castings to be austempered are usually alloyed with some Ni and Mo. The treatment starts with austenitizing. The rapid cooling which follows is not to room temperature but to between 500 and 900°F (262-482°C). The piece is held isotermally (usually in a salt bath) until after the austenite-bainite transformation is complete.

Typical hardness value obtained in this process are from 275 to 375 BHN, the higher the lower the temperature of the isothermal hold. The latter is followed by aircooling.

vi)   Incomplete austempering

This heat treatment is a recently developed one from Finland. The S.G. iron produced in this process possesses high strength and ductility. Ultimate strength-elongation values obtainable are in the incredible range of upto 155000 PSI (1,068 N/mm^2) with 10% elongation. In order to avoid pearlite from forming upon quenching, a minimal amount (about 0.25%) of molybdenum is used. To avoid ferrite, a slight alloying with copper (0.7%) or nickel (to 2.5%) is used. Ni also helps to avoid pearlite.

The casting is first austenitized, then quenched in a salt bath from 1650°F (900°C) to 900°F (370°C). After some time, the austenite-bainite transformation begins. It never comes to completion, however, because the austenite, quenched from a high temperature contains nearly 1% carbon and this high carbon content

stabilizes austenite (prevents martensite formation) to or below room temperature. The matrix structure consists of bainite and austenite.

vii) Quenching and Tempering Annealed S.G.iron

In this treatment S.G. iron is first completely annealed. After this, it is reheated to within the critical transformation temperature range (Fig. 4). Now an oil or water quench is applied. After this step the structure consists of ferrite and martensite. Finally, the martensite is tempered at a relatively high temperature of 1200^0F (650^0C).

S.G. iron heat treated in this way will approximate the impact resistance of a ferritic S.G. iron, and the strength of a fully pearlite one.

CHAPTER - 3

EXPERIMENTAL PROCEDURE

3 1 Ladle Preparation:

A special type of ladle (fig. 2) was designed and constructed for proper spherodization. The ladle was designed in such a way so that the height of the ladle was twice its diameter approximately. The height and diameter of the prepared ladle used in this project work were 26 cm and 16 cm respectively. At first the ladle was fabricated with mild steel sheet and then the lining of 4 cm thickness was made inside the ladle with refractory materials.

In order to keep spheroidizer (FeSiMg) into the bottom of the ladle a partition of 6 Cm height and 1.5 cm thickness was designed at the bottom portion of the ladle.

A special type of lid was made with refractory globules to cover the ladle (fig. 2).

An inclined hole with proper slope was made on the lid in order to pour molten metal into the ladle.

3.2 Preparation of circular steel sheet

A number of circular sheets made of mild steel sheet of 1/8" thickness and 12.5 cm diameter were cut in order to cover the master alloy (FeSiMg) inside the ladle for delaying the reaction of Mg alloy with the iron melt.
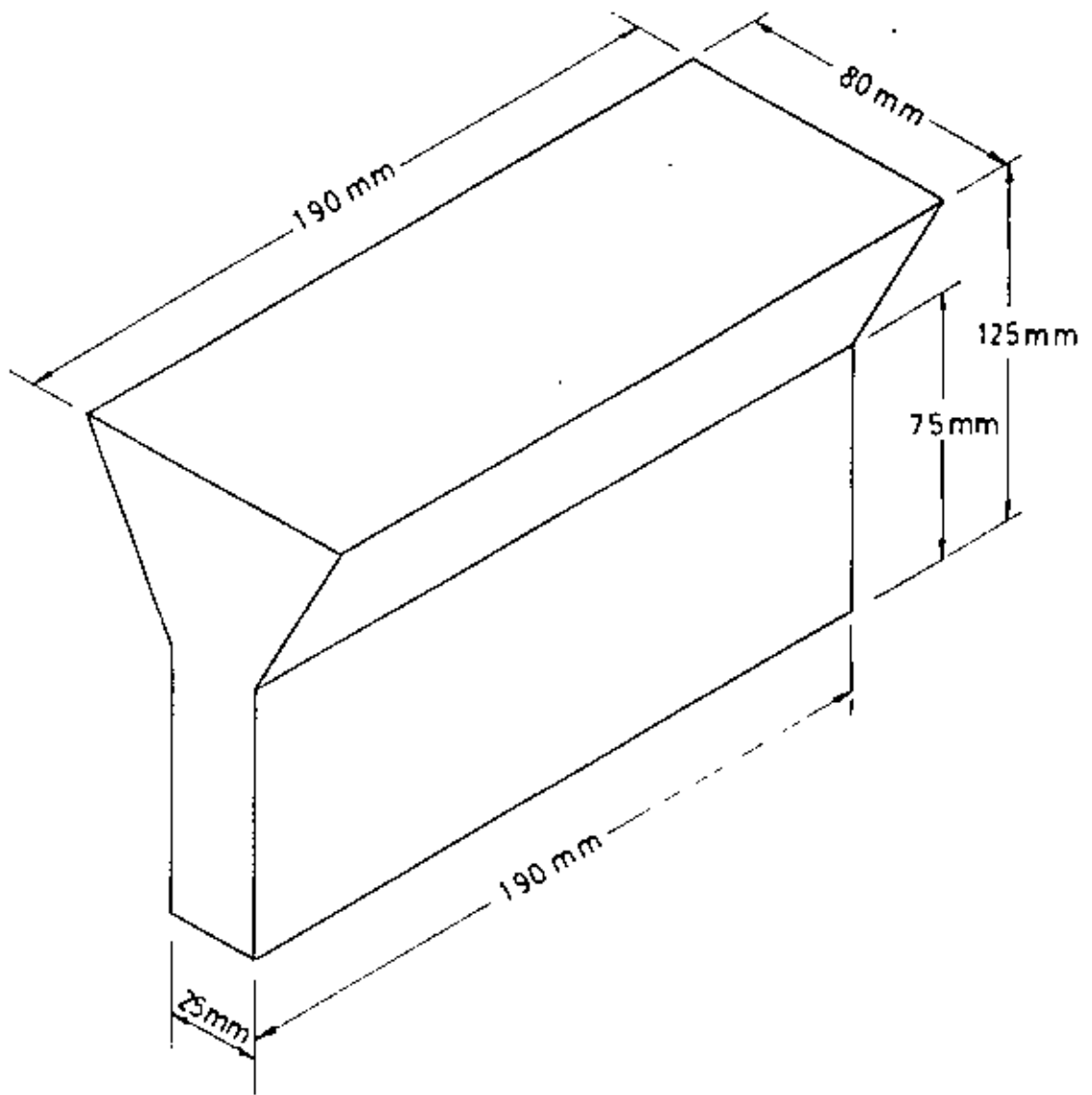
Fig. 6   Y - block casting

3.3 Mould Preparation

.   A few moulds were prepared for casting of keel blocks having standard size (Fig 6). Then the moulds were properly heated with burner to remove moisture form the lining. A few moulds were also prepared for casting of bars having different diameters.


3.4 Chemical analysis of Pig iron and mild steel rod.

Pig iron and mild steel rods are the main raw materials used to manufacture S.G. iron. The percentage of Carbon, Silicon, Manganese, Sulphur and Phosphorous contents of Pig iron and the carbon, Silicon, Sulphur, Phusphorous and Manganese contents of mild steel were determined by standard methods of chemical analysis.

3.5 Charge calculation

Charge calculation was carried out in order to maintain the desired percentage of carbon and silicon in S.G. iron which has been shown in Table 3, 5, 9 and 11.

The required amount of CaC_2 used to reduce the sulphur content of the charge from 0.12 to 0.01% was calculated on the basis of the following reaction:

$Fes + CaC_2 + O_2 = Cas + Fe + 2Co.$
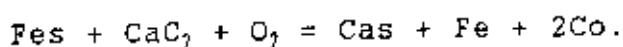
The amount of FeSiMg and inoculant required to produce S.G. iron from 17.272 kg desulphurized charge in the 1st heat were calculated which has been shown in table-5. Charge calculation for

desulphurization and production of S.G. iron in the 2nd heat have been shown in table 9 and table 10 respectively.

3.6 Desulphurization

In order to eliminate or reduce the sulphur content of pig iron and mild steel rod to a very low level, the desulphurization was carried out. Pig iron and mild steel rods of proper proportion were charged into an induction furnace. The furnace was then switched on. When the charge was sufficiently melted, a suitable amount of flux was added into the furnace to clean the molten metal. The slag was then removed from the top of the furnace with a scraper. The furnace was then tilted and the molten iron was poured into a pre-heated ladle/graphite crucible. During pouring of molten metal into the crucible a controlled amount of granulated CaC_2 of about 5 mm size were then continuously added into the stream of liquid iron. As soon as the pouring was stopped, the liquid metal in the ladle was stirred with the help of a mild steel rod in order to ensure thorough reaction of CaC_2 with the sulphur present in the liquid iron. The sulphide slag which floated on the top of the liquid iron, was then removed by a scraper. CaC_2 reacts with sulphur in iron as follows: $CaC_2 + FeS + O_2 = CaS + Fe + 2Co$. This slag (CaS) Causes to produce acetylene gas which comes in contact with moisture and may result in fire hazard in the atmosphere. So the slag was taken away quickly from the foundry shop and immersed into a water tank. After desulphurization the liquid iron was poured into a metal mould to produce small pigs or pig of suitable size,

which could be subsequently used for the production of S.G. iron.

This desulphurized pig was then analysed for the determination of C, Si, Mn, S & P.

3.7 Production of S.G. iron

The produced desulpherized iron was used for the production of S.G. iron. The weighed amount of desulphurized iron was placed into the induction furnace and the furnace was switched on. When the charge was sufficiently molten, flux was added into the furnace to make sufficient slag. The slag was then removed by means of a scraper and the temperature was measured to be about 1400^0C with the help of a pyrometer. The temperature of the molten metal inside the furnace was raised to the superheating temperature of about 1592^0C.

In the first heat, spherodizing element (FeSiMg) and inoculant (FeSi) were placed into the bottom pocket of the pre-heated specially prepared ladle. The pocket was then covered with a spherical mild steel sheet. The ladle was covered with a specially prepared lid and the cover was clamped with the ladle. The covered ladle was then brought to the induction furnace. When the superheating temperature was reached, the furnace was tilted, slag was removed and then molten metal was poured into the specially prepared ladle through the hole on the ladle cover at the superheating temperature. The reaction between molten metal, FeSiMg and FeSi was taken place. When the reaction was completed, the cover was removed and flux was added and slag was removed. The
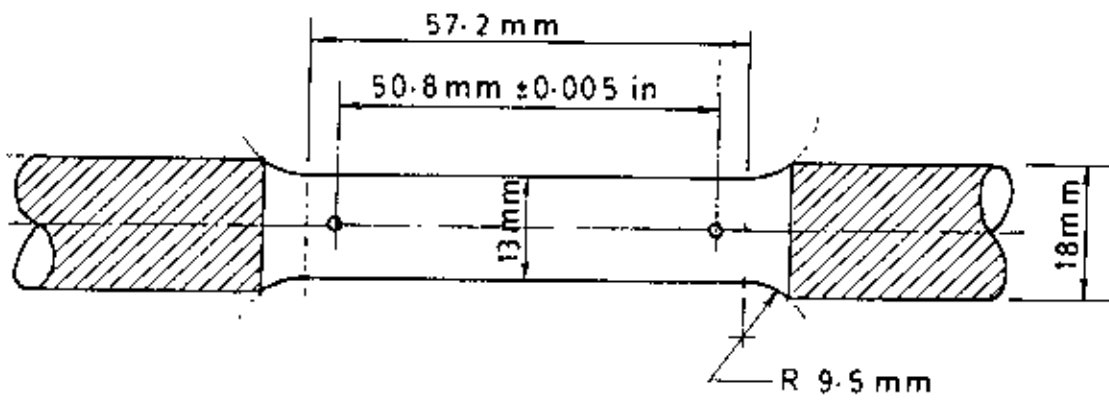
57.2 mm

50.8mm ±0.005 in

13 mm

18 mm

R 9.5 mm

Fig. 7　Specimen for tensile test

R 0·25mm
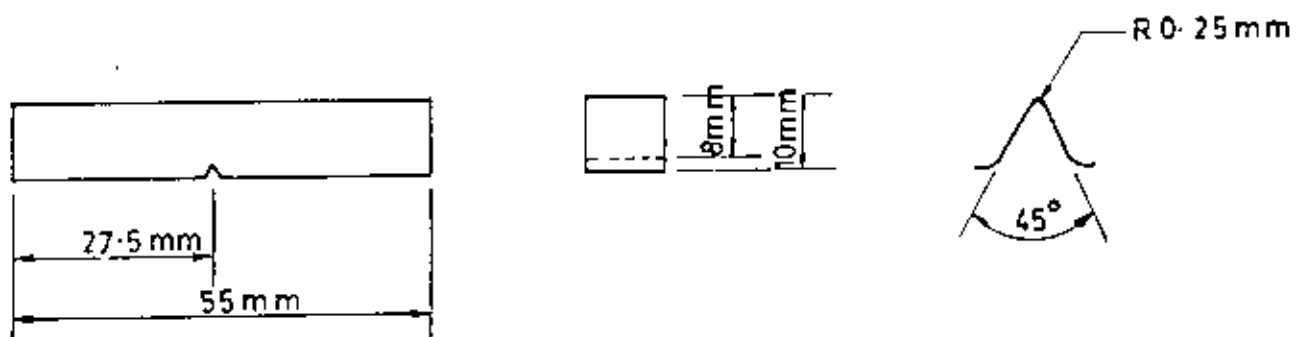
27·5 mm

55 mm

8 mm

10 mm

45°

Fig. 8 Charpy V-notch specimen

molten metal was then poured into the mould from the ladle and allowed to cool slowly.

In the 2nd heat, only spherodizer was placed into the bottom pocket of the pre-heated ladle. After spherodizing treatment, the cover of the ladle was removed and flux was added and slag was removed. Then the inoculant, FeSi, was added into the ladle and stirred with a mild steel rod. The molten metal was then poured into the mould from the ladle and allowed to cool slowly.

Moulds were broken down after slow cooling for one day. The cast rods of different diameters and keel blocks were cleaned with a metallic brush.

3.8 Chemical analysis of S.G. iron

Turnings of S.G. iron were collected for chemical analysis. The percentages of C, S, Si, P, Mg and Mn contents of the S.G. iron were determined by standard methods of chemical analysis.

3.9 Preparation of specimens for different test

Specimens from circular rods of different diameters produced in the 1st heat were cut for metallographic test.

Standard tensile specimens with a nominal diameter and minimum parallel length of $\frac{1}{4}$" and $2\frac{1}{4}$" respectively (shown in Fig. 7) were prepared from keel blocks produced in the 1st and the 2nd heats for tensile test.

Standard charpy V-notch impact test specimens (Fig.8) were

also prepared as per British Standard Specification from keel blocks for impact test.

3.10 Heat treatment

Specimens cut from bars having different diameters were annealed at $950^{0}C$ for 1 hour. A few legs of keel blocks were also annealed at $950^{0}C$ for 1 hour. Then tensile specimens and Charpy V-notched impact specimens were prepared from these legs of keel blocks.

3.11 Metallographic test of circular bars

In order to examine the effect of cooling rate on the morphology of graphite, nodule count, nodularity and matrix of S.G. iron produced, the specimens cut from different bars of different section sizes were polished roughly by means of grinding. Then the specimens were smoothly polished successively by means of polishing papers ranked 3, 2, 1, 0. 2/0, 3/0, and 4/0. Finally the specimens were polished finely by means of buffing wheels using gamma aluminium oxide powder of varying fineness.

After polishing the specimens were cleaned by acetone. Microstructures of these specimens were examined under the optical microscope both in the etched and unetched conditions. Photographs of microstructure were taken as necessary.

3.12 Mechanical test of tensile specimens

As-cast and annealed tensile specimens were tested with a tensile testing machine to obtain data of ultimate tensile strength, % elongation and % reduction in area.

3.13 Hardness and metallographic tests of the as-cast tensile specimens.

After tensile test, specimens were cut from broken end of tensile specimens for hardness and metallographic tests. The hardness of the specimens were measured in the B scale by means of a rockwell hardness tester.

The microstructures of the broken ends of tensile specimens were examined under the optical microscope and photographs of micro-structures were taken.

3.14 Mechanical test of V-notched charpy specimens

V-notched Charpy specimens having 55 mm length and 10 mm cross section (Fig. 8) were prepared from keel blocks produced in the 2nd heat. These specimens were tested by means of an universal impact testing machine under the as-cast and annealed conditions.

CHAPTER-4

EXPERIMENTAL RESULTS

4.1 Chemical analysis of pig iron, and mild steel rod

The composition of pig iron and mild steel rods used as charging materials for the production of S.G. iron were determined by standard methods of chemical analysis. The compositions of the pig iron and the mild steel rods obtained are listed in table-2. It is found from this chemical analysis that the pig iron used as charging material for the production of S.G. iron contains high S and Mn. Charge calculations for desulphurization shown in table-3 was followed on the basis of chemical analysis of pig iron and mild steel rod.

4.2 Chemical analysis of desulphurized iron

To ensure the desired composition of desulphurized iron, the percentage of C, Si, Mn, S & P were determined by standard method of chemical analysis. The results of chemical analysis of the desulphurized iron produced in the 1st heat is shown in table-4. The compositions of desulphurized iron produced in the 2nd heat were also determined which has been listed in table-11.

It is found that the analysis of both of the desulphurized iron samples shows approximately the same result with the exception of C content.

4.3 Chemical analysis of S.G. iron produced

In order to ensure the desired composition the S.G. iron produced in both the 1st and the 2nd heats were chemically analysed. The results of the analysis of S.G. iron produced in the 1st and the 2nd heats are listed in table-6 and table-12 respectively. Table-6 shows that the carbon content of the S.G. iron produced in the 1st heat is 3.05% which is lower than the desired composition. But table-12 shows that the carbon composition of the S.G. iron produced in the 2nd heat is exactly which had been desired.

4.4 Microstudy

4.41 Microstudy of circular bars having different diameters

Microstructures of the specimens cut from circular bars of different diameters were observed under the optical microscope in the etched and the unetched conditions. Photographs of microstructures were taken.

Fig. 9(a) shows the microstructure of a bar having $\frac{1}{2}$" diameter under the etched condition. Little spheroidal graphites are found in the microstructures. Few vermicular graphites are also observed in the microstructure. Microstructures of the etched specimen of $\frac{1}{2}$" diameter bar (Fig. 9.b) shows that the matrix contains pearlite and cementite. The matrix consisted of 55% pearlite and 45% cementite approximately. Fig. 9(c) shows the microstructure of the same bar under annealed condition. In the microstructure of unetched specimen little spheroidal graphites were found. Few vermicular

graphites are also observed. Microstructure of etched specimen of this annealed bar (Fig. 9.d) shows all ferritic matrix.

Spheroidal graphites were found in the microstructure of the specimen of 3/4" diameter bar shown in Fig.10a. Few vermicular graphites were also observed in the microstructure. Relatively larger and more nodules than previous ones were observed in this microstructure. The microstructure of this specimen under etched condition shown in Fig.10b, showed that the matrix contained pearlite and cementite. The percentage of cementite in the matrix was observed as 30%. The rest was the pearlite. Fig. 10(c) shows the microstructure of the same bar under annealed condition. In the microstructure of unetched specimen spheroidal graphite and very few vermicular graphite were observed. The microstructure of the annealed specimen under etched condition shown in Fig. 10(d) showed that the matrix contained all ferrite.

Fig.11a and Fig.11b show the microstructures of the specimen of 1" diameter bar under unetched and etched condition respectively. Relatively large spheroids were found in the microstructures. Few nonspheroidal and vermicular graphites were also observed in the microstructure. More pin like little spheroids were found in this microstructure. Microstructure of etched specimen showed that the matrix contained pearlite and cementite. 20% cementite and 80% pearlite were found in this microstructure. Fig. 11c shows the microstructure of the same bar under annealed condition. In the microstructure of unetched specimen spheroidal graphite were found. The microstructure of this annealed specimen

under etched condition shown in Fig. 11d showed that the matrix contained ferrite and pearlite. The matrix consisted of 96% ferrite and 4% pearlite.

Relatively larger nodules were found in the microstructure of the specimen of 1½" diameter bar under unetched condition shown in Fig.12a. Few nonspheroidal graphites were observed in the structures.

Pin like little spheroids were found to increase in this microstructure than previous ones. The microstructure of the specimen of the same bar under etched condition (Fig. 12b) showed that the matrix contained 91% pearlite, 7% cementite and 2% ferrite. Fig.12c shows the microstructure of the same bar under annealed condition. In the microstructure of unetched specimen spheroidal graphites were observed. The microstructure of this annealed specimen under etched condition shown in fig. 12d, showed that the matrix contained pearlite and ferrite. The matrix consisted of 94% ferrite and 6% pearlite.

Fig. 13a shows the microstructure of the specimen of 2" diameter bar under unetched condition. It revealed that the microstructure contained larger spheroidal graphite than those of previous bars. More pin like little spheroids were found in this structure than those in the structure of previous ones. Mainly spheroidal graphites were found in the microstructure. A few vermicular and chunk graphites were also found in this microstructure. Microstructure of the same specimen under etched condition (Fig.13b) revealed that the matrix contained 96% pearlite

and 4% ferrite. Ferrites were observed as rings round the nodules. Fig. 13c shows the microstructure of the same bar under annealed condition. In the microstructure of unetched specimen spheroidal graphites were observed. The microstructure of the annealed specimen under etched condition shown in fig. 13d showed that the matrix contained pearlite and ferrite. The matrix consisted of 92% ferrite and 8% pearlite.

Fig. 14a and Fig. 14b show the microstructures of $2\frac{1}{2}"$ diameter bar under unetched and etched condition respectively. Fig. 14a shows that the microstructure contains larger spheroidal graphites than previous microstructures. Many pin like little spheroids were found in this structure. A few vermicular graphites were formed with spheroidal graphite in the structure. Fig 14b reveals that the matrix contains 92% pearlite and 8% ferrite.

The results of this microstudy of bar having different diameters are listed in table-7. Fig. 14c shows the microstructure of the same bar under annealed condition. In the microstructure of unetched specimen spheroidal graphites were observed. The microstructure of the annealed specimen under etched condition shown in Fig 14d, showed that the matrix contained pearlite and ferrite. The matrix consisted of 90% ferrite and 10% pearlite.

4.42 Microstudy of tensile specimens

Microstructures of tensile specimens cut from Keel blocks produced in the Ist and the 2nd heat were observed. Photographs were taken. The results of microstudy of tensile specimens of keel

blocks produced in the Ist and the 2nd heat are listed in table 8 and table 13 respectively.

Three numbers of tensile specimens were prepared from keel block "A" produced in the Ist heat. After tensile test, specimens were cut from each tensile specimen for metallographic test.

Two specimens were cut from B_1 keel block and two were cut from B_2 keel block produced in the 2nd heat. Microstructures of specimens of each keel block were observed under the as-cast and the annealed condition.

The microstructure of specimen A_1 under unetched condition is shown in fig 15a. Comparatively slight large nodules were found in this microstructure. Few chunk graphites were also found in this microstructure. The etched microstructure of this specimen shown in fig 15b showed that it contained 10% ferrite, 1% cementite and 89% pearlite. Most of these ferrites were found as rings round the nodules.

Microstructure of A_2 specimen under unetched condition shown in fig 15c showed that it contained more nodules in comparison with the microstructure of A_1 specimen. More pinlike little spheroids were also found in this microstructure. The microstructure of this specimen under etched condition (Fig 15d) showed that the matrix contained pearlite, ferrite and cementite. The percentage of pearlite, ferrite and cementite were found as 84%, 15% and 1% respectively.

Fig 16a and Fig 16b show the microstructures of specimen A_3 under unetched and etched conditions respectively. In this

microstructure, the number of nodules were found to be increased slightly than previous one. Pin like little spheroids were also found in this microstructure. The microstructure of this specimen under etched condition (Fig 16b) showed that the matrix contained 84% pearlite, 15% ferrite and 1% cementite.

Microstructures of tensile specimens cut from B_1 and B_2 keel blocks produced in the 2nd heat are shown in Fig 17 to Fig 18. Fig 17a shows the microstructure of as cast B_{11} tensile specimen under unetched condition. More numbers of nodules, better nodularity, and more uniform distribution of nodules were found in this microstructure compare to the microstructure of tensile specimens produced in the 1st heat. The microstructure of this as-cast specimen under etched condition (Fig 17b) showed that the matrix contained 59% pearlite, 30% ferrite and 1% cementite.

Fig 17c shows the microstructure of annealed specimen B_{12} cut from B_1 keel block under unetched condition. It was found that the microstructure of as cast (Fig 17a) and annealed (Fig 17c) specimens under unetched condition were looked alike. But the microstructure of annealed tensile specimen B_{12} under etched condition (Fig 17d) showed that the matrix contained only ferrite.

The microstructure of as cast tensile specimen B_{21} cut from B_2 keel block under unetched condition is shown in fig 18a. It was found from this microstructure that nodules of lower numbers and of larger sizes were formed in keel block B_2 compare to keel block B_1. The microstructure of this specimen under etched condition (Fig.

18b) showed that the matrix contained 69% pearlite, 30% ferrite and 1% cementite.

Fig 18c shows the microstructure of annealed B_{22} specimen cut from B_2 keel block under unetched condition. This micro-structure was the same as the microstructure of the specimen under as-cast condition (Fig 18a). But the etched microstructure of this annealed specimen (Fig 18d) showed that the matrix contained only ferrite.

4.43 The count of nodules and the measurement of nodularity from the microstructure

The number of nodules formed per square milimetre were count and the percentage of nodularity was measured from the microstructure of tensile specimens and bars having different diameters.

The result of nodule count and nodularity measurement of circular bars having different diameters is listed in table-7.

The number of nodules observed per square milimetre in the microstructure of 1/2" diameter bar under as-cast condition (Fig 9a) were count in the range of 15-50 nodules per mm^2. The average nodularity of nodules of this microstructure was measured as 92%. The number of nodules observed per square milimetre of the microstructure of 1/2" diameter bar under annealed condition (Fig 9c) were count in the range of 275-300 nodules per mm^2. The average nodularity of nodules of this microstructure was measured as 42%.

The number of nodules observed per square milimetre in the microstructure of 3/4" diameter bar (Fig 10a) were count in the

range of 50-75 nodules per mm^2. The average nodularity of nodules of this microstructure was measured as 88%. The number of nodules observed per square milimetre in the microstructure of 3/4" diameter bar (Fig 10c) were count in the range of 200-225 nodules per mm^2. The average nodularity of nodules of this microstructure was measured as 89%.

The number of nodules observed per square milimetre in the microstructure of 1" diameter bar (Fig 11a) were count in the range of 75-100 nodules per mm^2. The average nodularity of nodules of this microstructure was measured as 84%. It was noted that pin like little spheroids were increased as the section sizes of bars were increased. As a result the total nodule count of thicker bars were found to be increased. The number of nodules observed per square milimetre in the microstructure of 1" diameter bar under annealed condition (Fig 11c) were count in the range of 125-130 nodules per mm^2. The average nodularity of nodules of this microstructure was measured as 84%.

The number of nodules observed per square millimeter in the microstructure of 1½" diameter bar (Fig 12a) were count in the range of 100-125 nodules per mm^2. The average nodularity of nodules of this microstructure was measured as 86%. The number of nodules observed per square milimetre in the microstructure of 1½" diameter bar under annealed condition (Fig 12c) were count in the range of 100-125 nodules per mm^2. The average nodularity of nodules of this microstructure was measured as 88%.

The number of nodules observed per square milimetre in the

microstructure of 2" diameter bar (Fig 13a) were count in the range of 125-130 nodules per mm^2. The average nodularity of nodules of this microstructure was measured as 88%. The number of nodules observed per square milimetre in the microstructure of 2" diameter bar under annealed condition (Fig 13c) were count in the range of 125-130 nodules per mm^2. The average nodularity of nodules of this microstructure was measured as 89%.

The number of nodules observed per square milimetre in the microstructure of 2½" diameter bar (Fig 14a) were count in the range of 130-140 nodules per mm^2. The average nodularity of nodules of this microstructure was measured as 87%. The number of nodules observed per square milimetre in the microstructure of 2½" diameter bar under annealed condition (Fig 14c) were count in the range of 130-140 nodules per mm^2. The average nodularity of nodules of this microstructure was measured as 87%.

The result of nodule count and nodularity measurement of tensile specimens cut from keel block A produced in the 1st heat is listed in table-8.

The number of nodules observed per square milimetre in the microstructure of specimen A_1 (Fig 15a) were count in the range of 100-125 nodules per mm^2. The average nodularity of nodules of this microstructure was measured as 87%.

The number of nodules observed per square milimetre in the microstructure of specimen A_2 (Fig 15c) were count in the range of 125-150 nodules per mm^2. The average nodularity of nodules of this microstructure was measured as 90%.

The number of nodules observed per square milimetre in the microstructure of specimen A_1 (Fig 16a) were count in the range of 150-175 nodules per mm^2. The average nodularity of nodules of this microstructure was measured as 92%.

The result of nodule count and nodularity measurement of tensile specimens cut from keel block B_1 and B_2 produced in 2nd heat is listed in table-13.

The number of nodules observed per square milimetre of the microstructure of specimen B_{11} (Fig 17a) were count in the range of 200-225 nodules per mm^2. The average nodularity of nodules of this microstructure was measured as 96%.

The number of nodules observed per square milimetre of the microstructure of specimen B_{21} (Fig 18a) were count in the range of 175-200 nodules per mm^2. The average nodularity of nodules of this microstructure was measured as 93%.

The number of nodules observed per square milimetre of the microstructure of the annealed specimen B_{12} (Fig 17d) were count in the range of 225-250 nodules per mm^2. The average nodularity of nodules of this microstructure was measured as 96%.

The number of nodules observed per square milimetre of the microstructure of the annealed specimen B_{22} (Fig 18c) were count in the range of 175-200 nodules per mm^2. The average nodularity of nodules of this microstructure was measured as 93%.

4.5 Measurement of mechanical properties by tensile test

The result of tensile test of specimens A_1, A_2 and A_3 cut from

keel block `A' produced in the 1st heat are listed in table-8. Ultimate tensile strength, percentage of elongation and percentage of reduction of area of A_1 specimen were measured as 450 N/mm^2, 2% and 7.69% respectively. Tensile test of specimen A_2 showed the ultimate tensile strength, percentage of elongation and percentage of reduction in area as 492 N/mm^2, 1.5% and 6.31% respectively.

Ultimate tensile strength, percentage of elongation and percentage of reduction in area of specimen A_3 were measured as 562 N/mm^2, 1% and 5.52% respectively.

The results of tensile test of specimens B_{11}, B_{21}, B_{12} and B_{22} cut from B_1 and B_2 keel block produced in the 2nd heat are listed in table-13.

Ultimate tensile strength, percentage of elongation and the percentage of reduction in area of as-cast B_{11} specimen were measured as 667 N/mm^2, 7% and 9.27% respectively. The tensile test of as cast specimen B_{21} showed that the ultimate tensile strength, percentage of elongation and percentage of reduction in area are as 544 N/mm^2, 3% and 3.15% respectively.

Ultimate tensile strength, percentage of elongation and percentage of reduction in area of annealed B_{12} specimen were measured as 508 N/mm^2, 23% and 29% respectively. The tensile test of annealed B_{22} specimen showed the ultimate tensile strength as 474 N/mm^2. This tensile specimen was broken under low load at the point outside the gauge length of the specimen. As a result the percentage of elongation and percentage of reduction of area could not be measured.

4.6 Measurement of impact energy of S. G. iron produced

V-notched impact specimens prepared from B_1 and B_2 keel blocks produced in the 2nd heat were tested by using the universal impact testing machine. Impact energy absorbed to break V-notch specimens prepared from B_1 and B_2 keel blocks produced in the 2nd heat were measured under the as-cast and the annealed conditions in NM unit which is shown in table-13.

Impact energy absorbed to break V-notch specimens B_{11} and B_{21} under the as-cast condition were measured as 80.75 NM and 80.00 NM respectively. The impact energy to break V-notch specimens B_{12} and B_{22} under annealed condition were measured as 75.20 NM and 75.50 NM respectively.

4.7 Measurement of hardness of tensile specimens

Hardness of tensile specimens prepared from keel block produced in both the 1st and the 2nd heat were measured in B scale of rockwell hardness tester. Rockwell hardness of specimen A_1, A_2 and A_3 are listed in table-7. The rockwell hardness in B scale of specimen A_1, A_2 and A_3 were found as 103, 102 and 104.

The result of hardness test of tensile specimens produced from keel block B_1 and B_2 is listed in table-13. The rockwell hardness in B scale of specimens B_{11} and B_{21} under as-cast condition were measured as 99 and 99.3. Under annealed condition, the rockwell hardness in B scale of specimen B_{12} and B_{22} were measured as 85 and 85.3 respectively.

CHAPTER - 5

DISCUSSION

5.1 Chemical analysis

Pig iron and mild steel rods were used to produce S.G. iron. Chemical analysis of pig iron as shown in table-2 showed that a high sulphur and manganese content were present in pig iron. Locally produced mild steel rod graded as SK-30 was also added as raw materials for the production of S.G. iron. Chemical analysis of mild steel rod showed that it contained low C, low S, low Si and low P which is shown in table-2.

Charge calculation was carried out in such a way (shown in table-3, table-5, table-9 & table-11) that the C.E. of the S.G. iron could be maintained at 4.17 level, but the chemical analysis of the disulphurized iron from the 1st heat (table-4) showed that it contained 3.3% carbon and 2.11% si. A carbon content of 3.41% was desirable in desulphurized iron. The carbon loss occurred due to the loss of powdered charcoal used as carburizer during the desulphurization and carburization treatment.

The chemical analysis of S.G. iron produced in the 1st heat (table-6) showed that it contained 3.05% carbon. The carbon loss occured during the melting and spheriodizing treatment of the desulphurized iron. As a result of this low carbon content, the C.E. value of the S.G. iron produced in the 1st heat was lowered.

The chemical analysis of desulphurized iron of the 2nd heat (table-11) showed that it contained 3.40% C. Other compositions

were found to be more or less the same as the compositions of desulphurized iron of the 1st heat. Chemical analysis of the S.G. iron produced in the 2nd heat (table-12) showed that it contained 3.21% C and 2.73% si. Carbon loss was found to be minimized due to the use of graphite rod instead of charcoal.

The percentage of si in the 2nd heat was also found to be increased slightly because of post-inoculation. Composition of other components were found to be more or less the same as the compositions of S.G. iron produced in the Ist heat.

5.2 Morphology of graphite, nodule count, nodularity and matrix of produced S.G. iron

Microstructures of tensile specimens cut from keel block and bars of different diameters produced in the 1st heat were observed. Micro-structures of tensile specimens cut from keel block cast in the 2nd heat were also observed under the optical microscope.

Fig 15a, Fig 15c and Fig.16a shows the microstructures of the tensile specimens A_1, A_2 and A_3 in the unetched condition respectively. Relatively lower nodule count and few chunk graphite were observed in these microstructures. Comparatively larger nodule sizes were seen in these structures. Low C.E. was responsible for this low module count. Another responsible factor in getting low nodule count and relatively larger nodule size was the inoculation process itself which was carried out inside the covered ladle with spherodizing treatment simultaneously during the 1st heat.

The effectiveness of inoculation sharply decreases with increasing temperature which is shown in Fig 3. So inoculation treatment should be done after the spherodizing treatment to avoid the fading effect.

Although A_1, A_1 and A_1 tensile specimens were cut from the same keel block "A", but relatively more nodules were found in the microstructure of the specimen A_1 (Fig 16a) in comparison to the A_1 and A_1 specimens, because this specimen was cut from the bottom part of the leg of keel block which solidified at a faster cooling rate compared to the top parts of the leg of the keel block.

It was found from the microstructures that a low C.E. and an inoculation treatment carried out simultaneously with spherodization had greater effect on the microstructure. The greater surface area to the volume ratio of the keel block caused it to cool considerably faster than the bar sections having a lower ratio studied in this work. For this reason the nodule count and nodularity in the microstructures of the keel block specimens were found to be better than those in the microstructures of the bars having thicker diameters.

In the 1st heat the keel block was poured at first and then the bars having different diameters (and 3" length each) were poured. Bars of $2\frac{1}{2}$", 2", $1\frac{1}{2}$", 1", 3/4" and $\frac{1}{2}$" diameters were poured successively after pouring the keel block. In general nodule count decreases and nodularity deteriorates as the section size increases. But in this work reverse fact was observed. The possible reason of this result is due to the fading effect of spherodization

and inoculation treatment. Since keel block was poured at first and then bars of thicker sizes to thinner sizes were poured successively. As a result the pouring temperature was gradually decreased during pouring of circular bars in the series of 2½" diameter to ½" diameter. Moreover the fading of spherodization and inoculation effect was obtained due to holding the treated iron for extended period of time during pouring of bars of different diameters. As a result comparatively low nodule count occured in thinner sections than thicker sections because the thinner sections were poured at low pouring temperature and with S.G. iron faded due to holding for extended period after spherodizing and inoculation treatment.

A large number of little spheroids were found in the microstructure of the thicker bars. Because of the presence of these little spheroids total nodule counts were increased. But the number of large-sized nodules were not found to be increased with the increase of section size. R.R. Kust and C.R. Loper[1] reported that the extended holding time during and after inoculation treatment resulted in pin like little graphite spheroid retention, particularly within the heavy section. It is found from the microstructures of unetched specimens of bars (Fig 9a, Fig 10a, Fig 11a, Fig 12a, Fig 13a and Fig 14a) a larger number of pin like little spheroids are found in the microstructure of heavy sections than in the microstructure of thin section.

It is noted that the microstructures of bar castings showed lower nodularity compared to the nodularity observed in the

microstructure of keel block castings. Due to the slow cooling rates of heavy section bars the liquid[5] will tend to redissolve a portion of the austenite shell, since austenite is not stable at these temperatures in these surroundings. Therefore spheroidal graphite may be exposed to the liquid and during further cooling deterioration of graphite occurs.

Studies of the effect of casting composition on the graphite structures in heavy section castings have shown[10] that castings poured from hypoeutectic melts contained coarse and irregular shaped graphite whereas true spheroids were obtained in hypereutectic melts in spite of longer solidification time.

Large size nodules in the microstructure of heavy section bars (Fig 11a, Fig 12a, Fig 13a, Fig 14a) were found to be coursed and irregular because of low C.E. of melt. The inoculation and magnesium treatments followed simultaneously inside the ladle in this casting. As a result less nodule count and lower nodularity were observed for not following the post-inoculation or mold inoculation. Although the microstructures of the heavy section bars contained a large number of pin-like little spheroids, but the nodularity of the large size of nodules in the heavier section bars were found to be lower.

It is also found that the size of nodules in the heavier section bars were comparatively larger than that in the thinner section bars. C. R. Loper and R. W. Heine[3] reported that large nodule size develops early during solidification, while the smaller size was dormant until a later stage. Growth of the spheroids to

large size occurs[5] during the eutectic arrest temperature. The growth of spheroids is selective, i.e. some grow to a large size, others remain dormant. The growth process in itself is diffusion-controlled, since the carbon to be precipitated as spheroidal graphite must pass through the protective austenite shell. A slower cooling rate allows a longer time for more graphite to develop. As a result the spheroidal graphites became larger in heavy sections.

The microstructures of tensile specimen A_1, A_2 and A_3 under etched condition (Fig 15b, Fig 15d and Fig 16b) showed that the matrix of these structures contained ferrite and pearlite. Ferrite, pearlite and cementite in different amounts were found in the microstructure of etched specimens of $2\frac{1}{2}$", 2" and $1\frac{1}{2}$" diameter bars (Fig 14b, 13b and 12b), but no ferrite rings were observed in the microstructure of unetched specimens of 1", 3/4" and $\frac{1}{2}$" diameter bars (Fig 11b, Fig.10b and Fig 9b). It is reported [1] that ferrite ring is formed by a diffusion process, the amount of ferrite formed should be a function of the cooling rate (section size), the composition of iron and the nodule count. So the tendency for the formation of ferrite ring increases with the increasing of section size. Slower cooling rate during solidification of thicker bars favoured the formation of ferrite rings.

It was found in this work that as the section size decreased, the number of nodules were decreased and the percentage of cementite in the matrix was increased. The main reasons of this result were the successive loss of pouring temperature, high Mn content in the charge and rapid cooling of thinner sections. In

general, the number of nodules are decreased following the increasing of carbide formation.

It is stated [9] that thin castings may safely be cast from S.G. iron with a carbon equivalent as high as 5. Lower pouring temperature also favours[3] carbide formation. As the holding time was increased and the pouring temperature was decreased, carbides appeared in the sample. Carbides were found in the microstructure of etched specimens (Fig 9b, Fig 10b, Fig 11b and Fig 12b). Fig 12b shows that a lesser no. of carbides are formed in this microstructure than in the microstructure of Fig 11b and the lesser no. of carbides are found in Fig 10b than in Fig 11b. Fig 9b shows that the matrix contains more cementite. So it is noted that carbides are more prone to form in the thinner sections where cooling rate is rapid. These carbides are rod like and massive (Fig 9b).

It is stated[21] that Mn is a moderately strong carbide promoter and must be limited for this reason. But in this work Pig iron used as charging material contained a high Mn content than the recommended level.

It has been demonstrated[22] that a nodule count of at least 430 nodules/mm^2 was required to ensure a carbide free structure in a 1/2 inch diameter bar. But in this work the nodule count from the microstructure of $\frac{1}{2}$" diameter bar was measured in the range of 15-50 nodules per mm^2 only. As a result excess carbides are found in Fig 9b because of the small number of nodules.

Bar having different diameters were annealed at 950⁰C for 1 hour and microstructures were observed under etched and unetched condition. Fig 9c, Fig 10c, Fig 11c, Fig 12c, Fig 13c and Fig 14c show the microstructures of ½", 3/4", 1", 1½", 2" and 2½" diameter bars under unetched condition respectively. It was found from these microstructures that the number of nodules and nodularity were slightly increased in thicker bars after annealing treatment. But annealed thin section bars having ½", 3/4" and 1" diameter (Fig 9c, Fig 10c, Fig 11c) contained larger number of nodules compare to the same bars under the as-cast condition. The number of nodules were found to increase gradually as the diameter of bars decreased. It was found from the Fig 9c, Fig 10c, and Fig 11c that the annealed specimens of ½", 3/4" and 1" diameter bars contained nodules in the range of 275-300, 200-225 and 125-130 per square milimetre respectively. Whereas the number of nodules in 1½", 2" and 2½" diameter bars were count in the range of 100-125, 125-130 and 125-130 per square milimetre respectively. Thinner bars under the as-cast condition contained lower number of nodules due to the formation of massive carbides. But the annealing treatment decomposed these as-cast carbides and more number of nodules were found to form in the ferrite matrix.

Fig 9d, Fig 10d, Fig 11d, Fig 12d, Fig 13d and Fig 14d show the microstructures of annealed bars having ½", 3/4", 1", 1½", 2" and 2½" under etched condition respectively. Due to the annealing treatment pearlite and cementite were dissolved and dispersed into the matrix as carbon particles resulting larger number of nodules.

It was found that the matrix of thicker section bars were not transformed into fully ferrite matrix after annealing treatment. Because the annealing treatment at 950^0C for 1 hour was not sufficient to transform all pearlite into ferrite. Whereas in thinner section bars this annealing treatment at 950^0C for 1 hour got sufficient time to transform all pearlite and cementite into ferrite matrix.

Because a lower carbon content was recorded in the S.G. iron produced in the 1st heat in which case charcoal had been used as Carburizer, graphite in the form of rods were used in the 2nd heat during the desulphurization and the carburization of melt. Moreover extra graphite amounting to 20% of the calculated graphite were added in order to take care of probable losses. Besides, post inoculation was carried out in ladle after magnesium treatment. The addition of graphite rods during desulphurization and carburization in the 2nd heat minimized the carbon loss of the melt. As a result large graphite volume was observed in the microstructure of S.G. iron produced in the 2nd heat compared to the S.G. iron produced in the 1st heat. In order to maintain proper pouring temperature the spheroidizing treatment was carried out at 1592^0C. C.E. meter was used to measure the C.E. in the 2nd heat. The C.E. meter showed a reading of 4.42 in this heat. Post-inoculation was carried out in a ladle after the spheroidizing treatment.

As a result of high C.E. of the melt and post inoculation, a larger nodule count and better nodularity were observed in the microstructure of tensile specimens produced in the 2nd heat.

It is reported[1] that S.G. iron structures are considerably improved if a practice of post-inoculation is followed after Mg. treatment has taken place. It is stated[17] that with a fixed C.E. of about 4.4 higher nodule counts could be obtained at high total si/low C combinations regardless of section sizes. It is also stated[1] that with the processing techniques and composition studied, 0.55% si addition as the post inoculant would be optimum when high nodule counts, good nodule distribution and nodule size are considered.

Two keel blocks were poured successively in the 2nd heat. B_{11} and B_{21} specimens were cut from B_1 and B_2 keel blocks respectively. It was found that the B_{21} specimen (Fig 18a) contained relatively lower nodule count and larger size nodules compared to B_{11} specimen (Fig 17a). This happened because the 2nd keel block was poured at a lower temperature in comparison to the 1st keel block.

The etched microstructures of B_{11} (Fig 17b) and B_{21} specimens (Fig 18b) showed that these contained more ferrite than that of the 1st castings. Comparatively more ferrite rings were found in the microstructure of tensile specimens produced in the 2nd heat due to post-inoculation.

The fading effect of inoculation was decreased and the total percentage of silicon in the S.G. iron was increased due to the post-inoculation. Enoukidze Nodar A, Lian Jinjiang, Zhong Weizhen, and Rong Yu[2] reported that the process of ferrite structure formation was highly developed with the increase of silicon content.
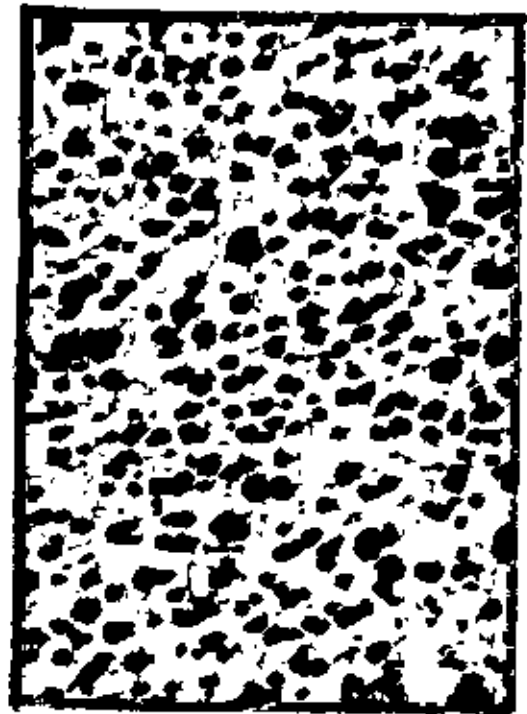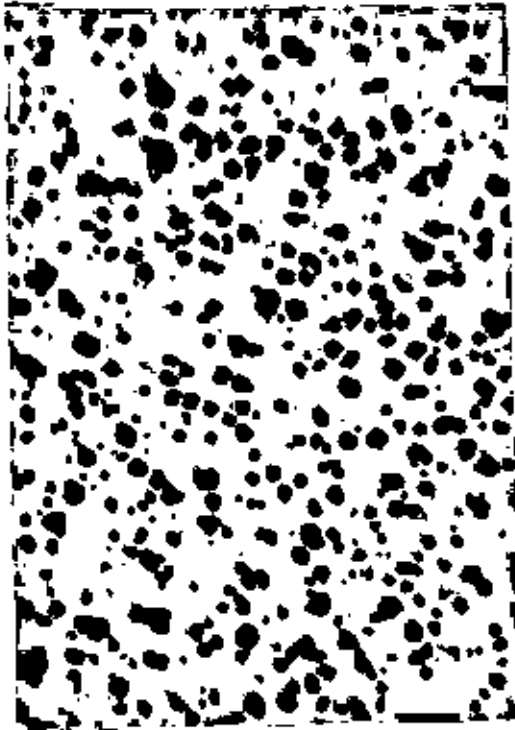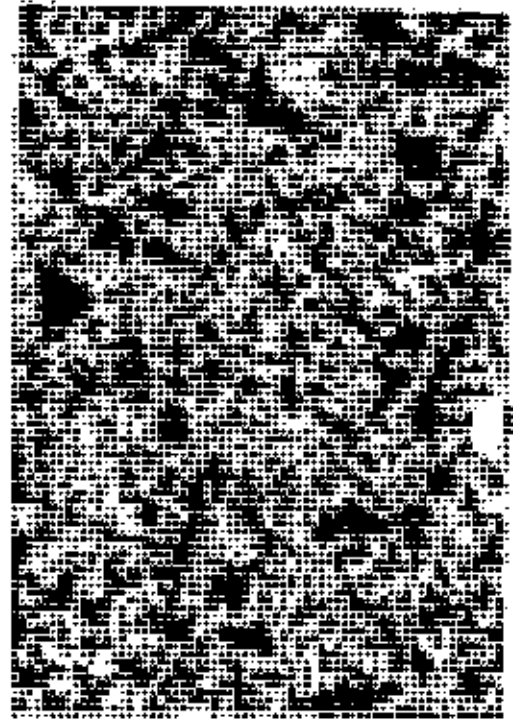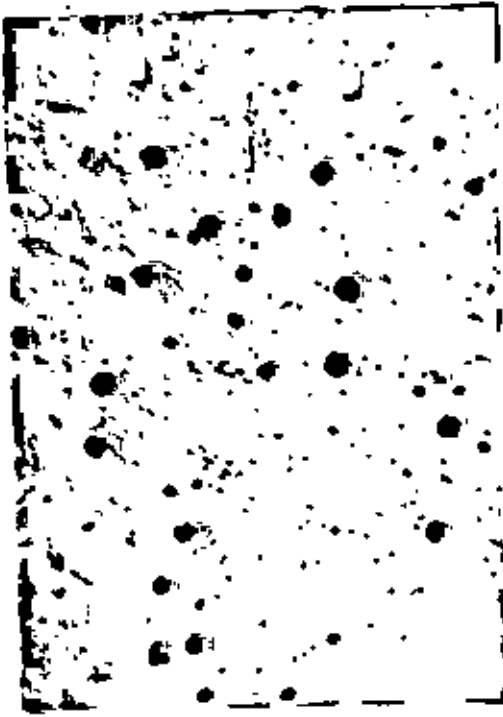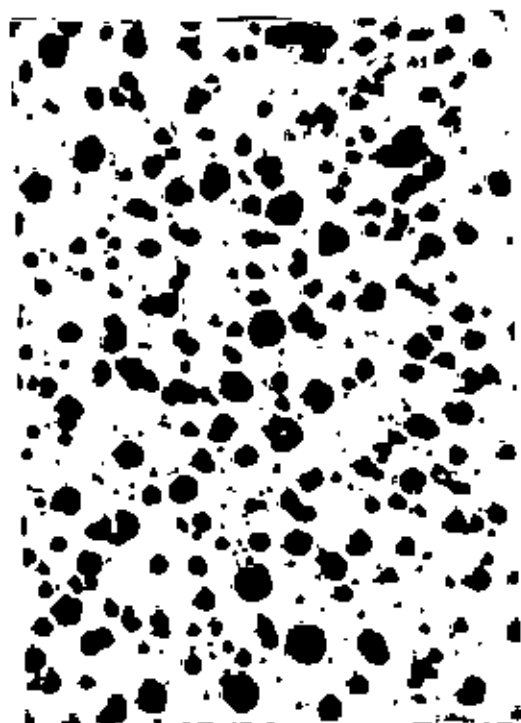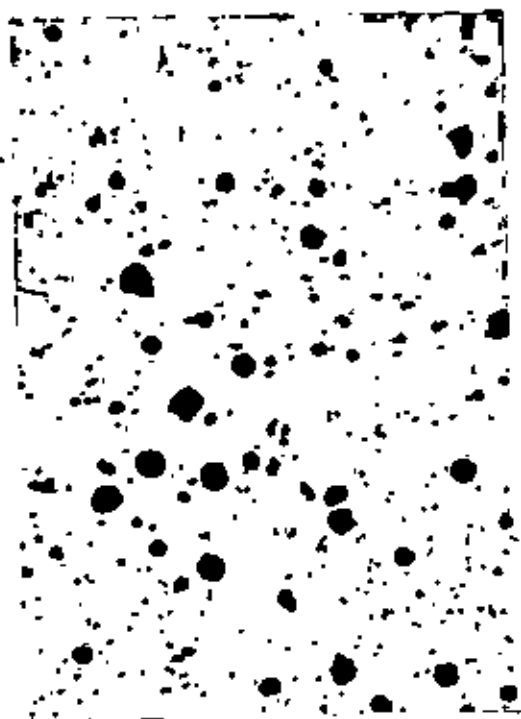
Fig 9:   Optical micrograph of ¼" diameter bar, x100:
    (a)   As–Cast, unetched
    (b)   As–Cast, etched
    (c)   Annealed at 950℃ for 1 hr., Unetched
    (d)   Annealed at 950℃ for 1 hr.. etched.

Fig 10: Optical micrograph of 3/4" diameter bar, x100:
- (a) As–Cast, unetched
- (b) As–Cast, etched
- (c) Annealed at 950°C for 1 hr., Unetched
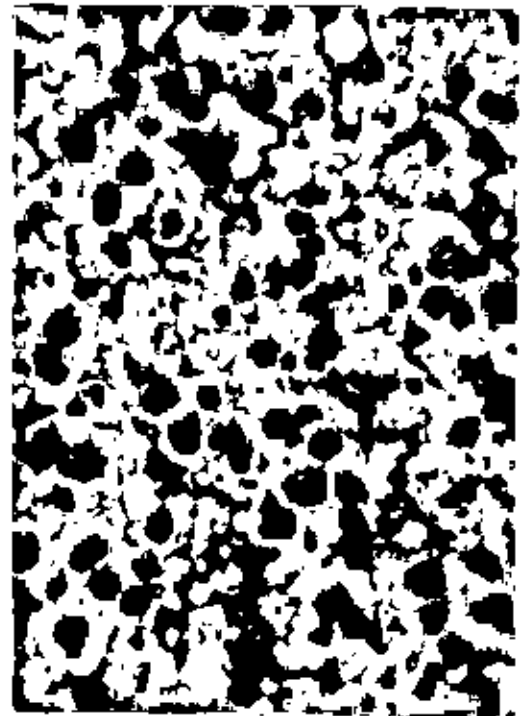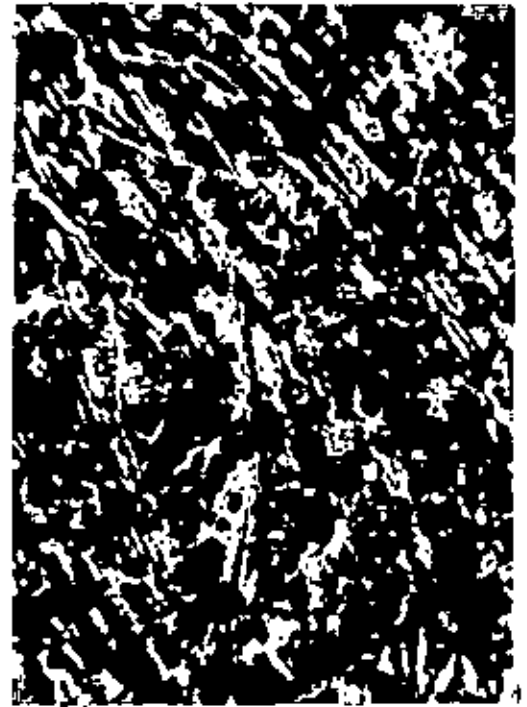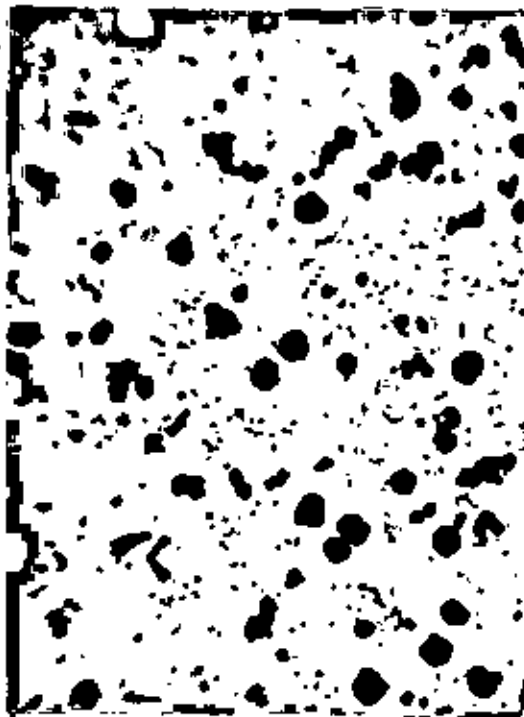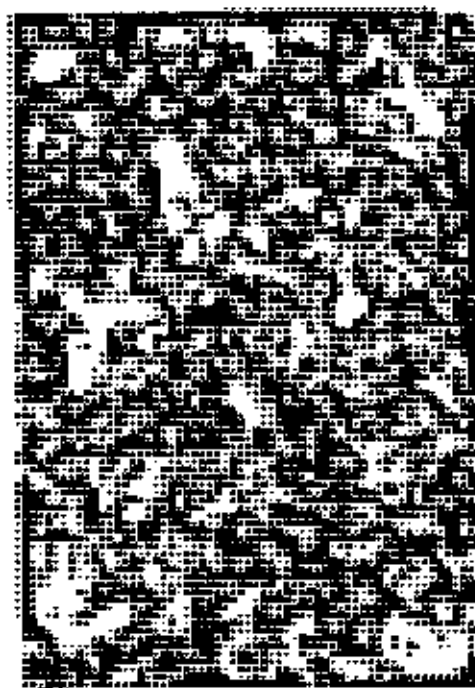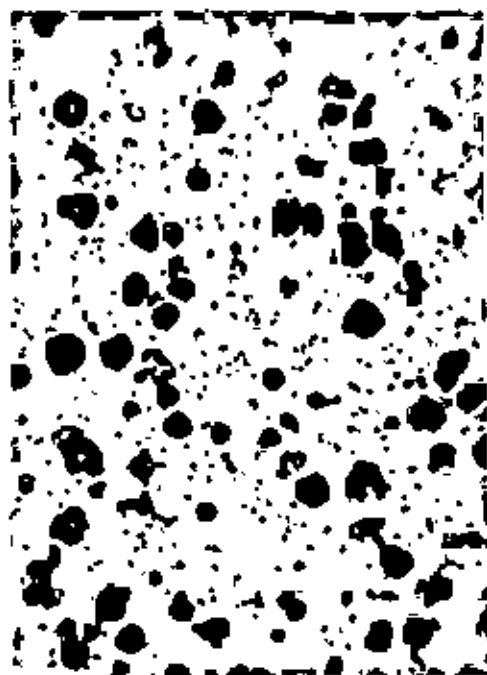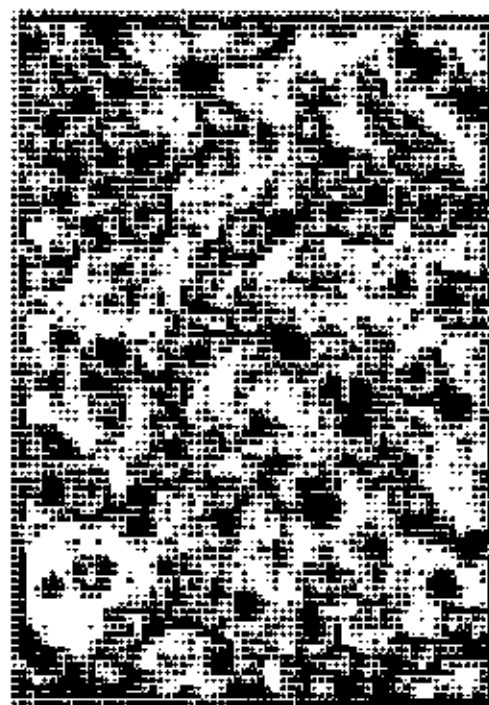- (d) Annealed at 950°C for 1 hr., etched.

Fig 11: Optical micrograph of 1" diameter bar, x100:
    (a)   As–Cast, unetched
    (b)   As–Cast, etched
    (c)   Annealed at 950°C for 1 hr., Unetched
    (d)   Annealed at 950°C for 1 hr., etched.
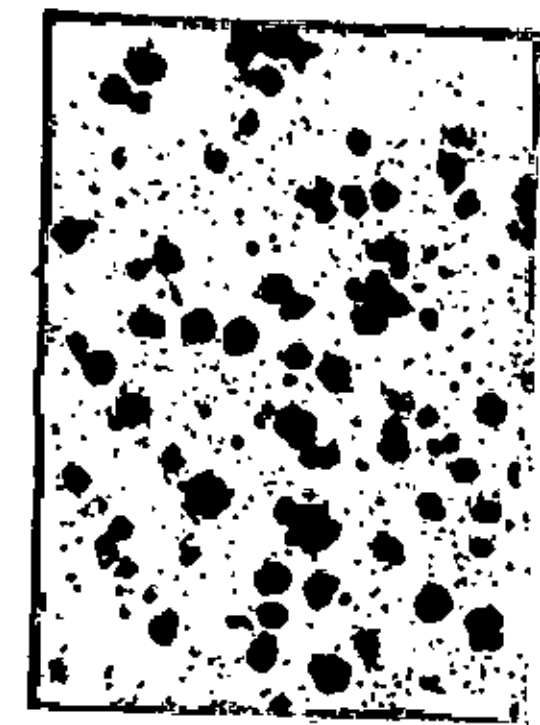
Fig 12: Optical micrograph of 1½" diameter bar, x100;
   (a)   As–Cast, unetched
   (b)   As–Cast, etched
   (c)   Annealed at 950°C for 1 hr., Unetched
   (d)   Annealed at 950°C for 1 hr., etched.

Fig 13: Optical micrograph of 2" diameter bar, x100:
(a)   As-Cast, unetched
(b)   As-Cast, etched
(c)   Annealed at 950°C for 1 hr., Unetched
(d)   Annealed at 950°C for 1 hr., etched.
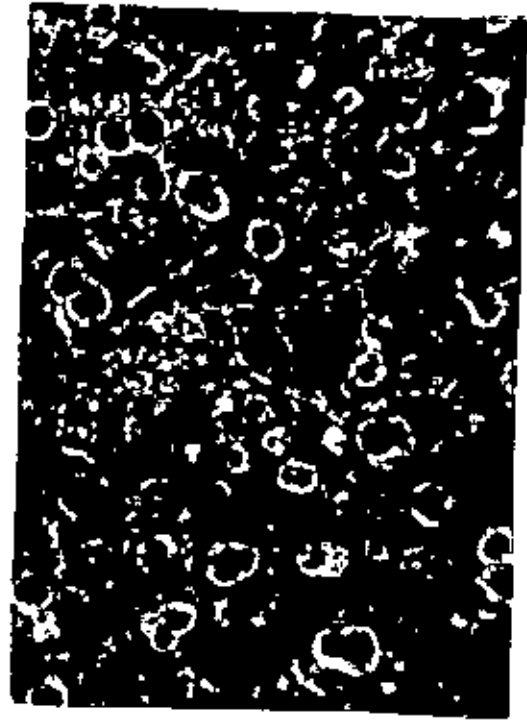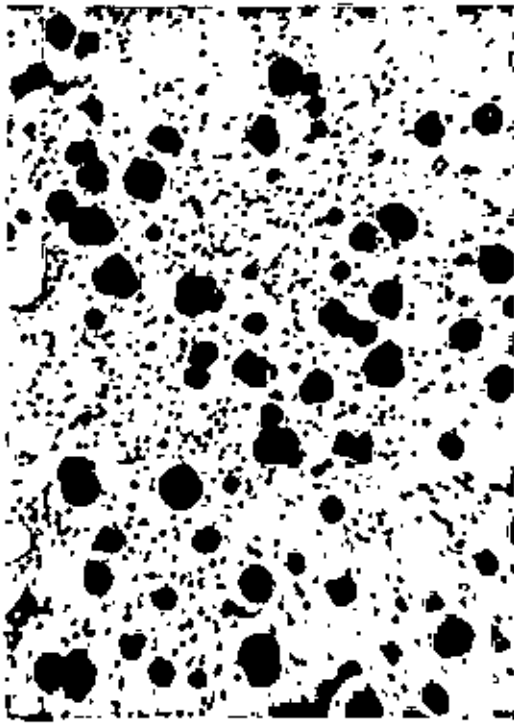
Fig 14: Optical micrograph of 2½" diameter bar, x100:
  (a)   As–Cast, unetched
  (b)   As–Cast, etched
  (c)   Annealed at 950℃ for 1 hr., Unetched
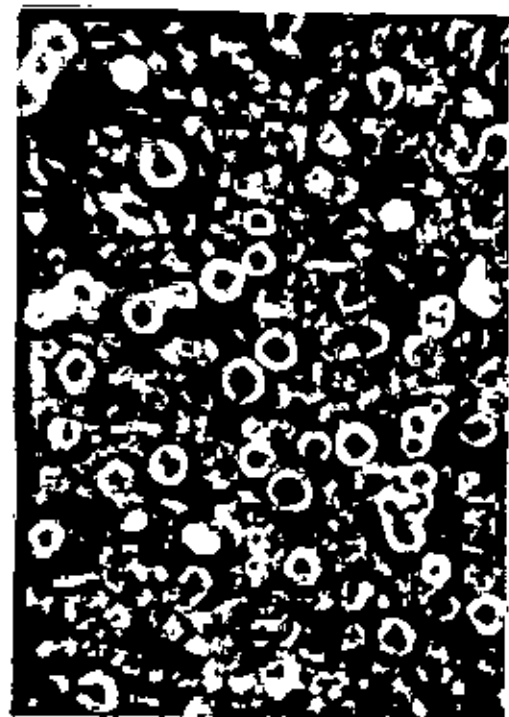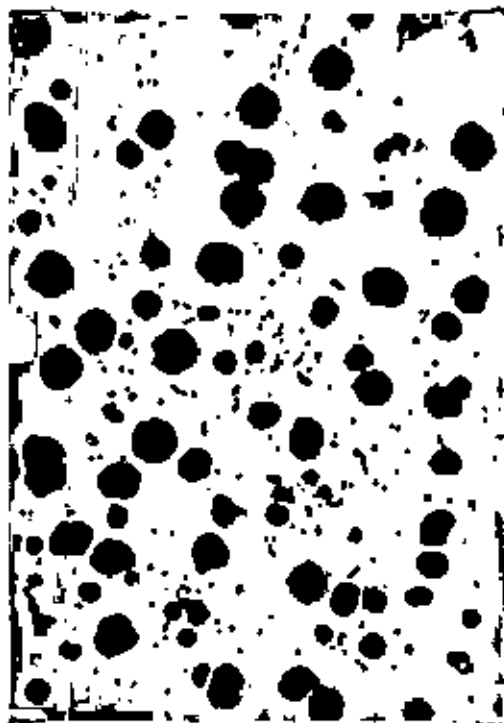 (d)   Annealed at 950℃ for 1 hr., etched.
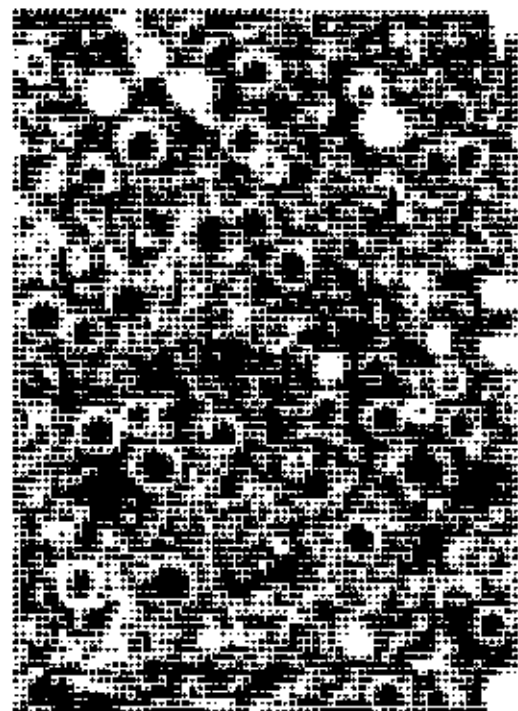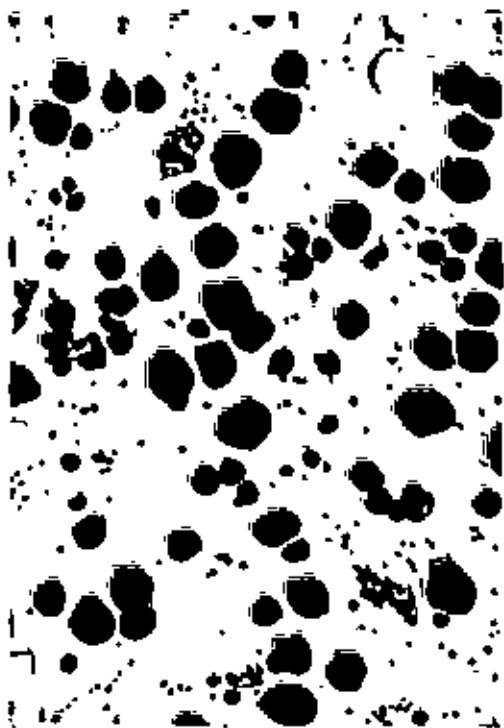
(c)   (d)

Fig 15:   Optical micrograph of tensile specimens produced in the Ist heat.
x100:

       (a)   As–Cast. Specimen A_1, unetched.
       (b)   As–Cast. Specimen A_1, etched
       (c)   As–Cast, Specimen A_2, unetched
       (d)   As–Cast, Specimen A_2, etched
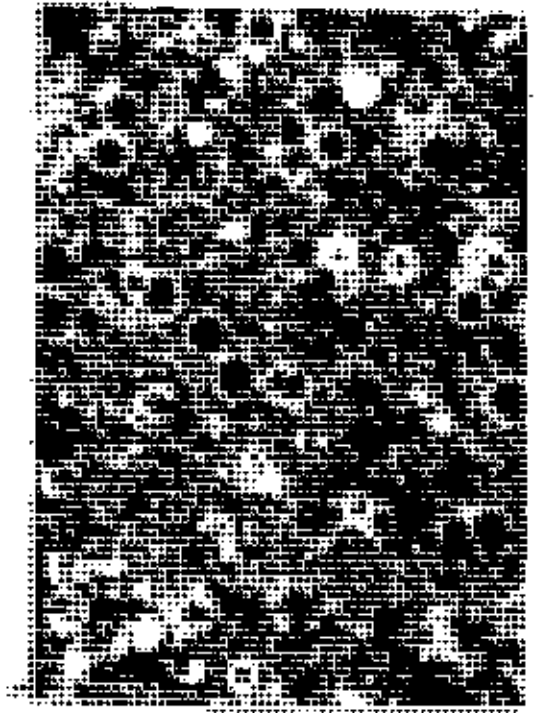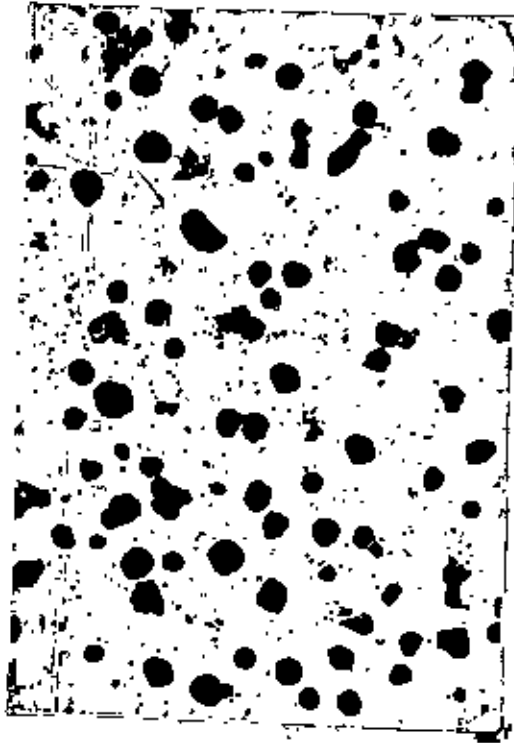
Fig 16:   Optical micrograph of tensile specimens produced in the 1st heat,
           x100:
           (a)   As-Cast, tensile specimen A₃, unetched.
           (b)   As-Cast, tensile specimen A₃, etched
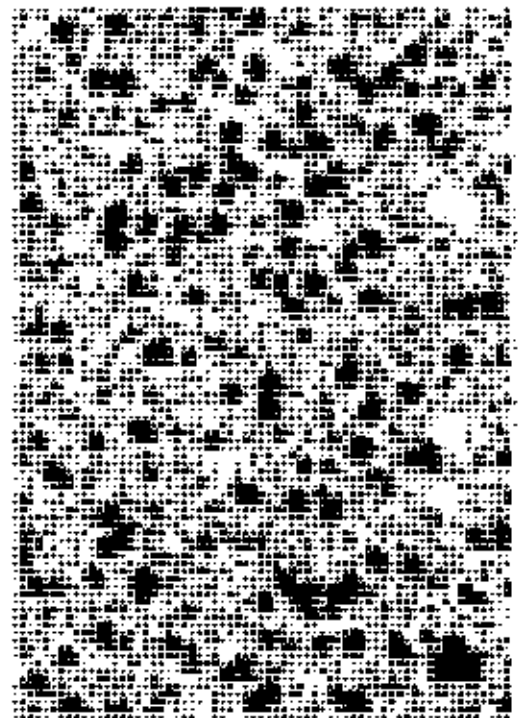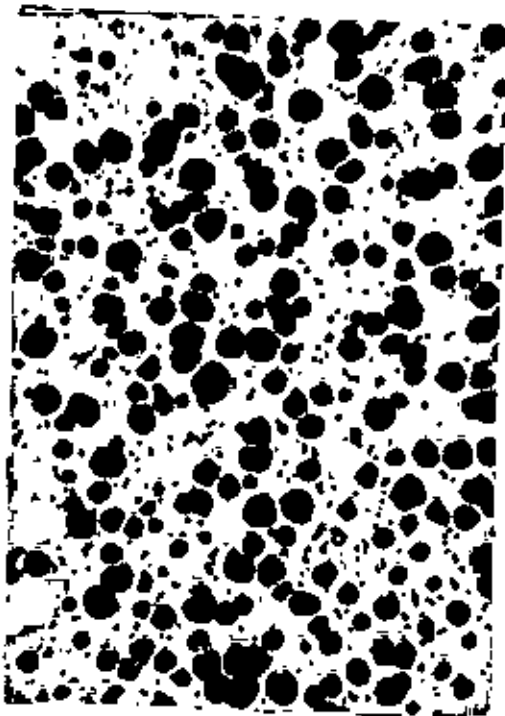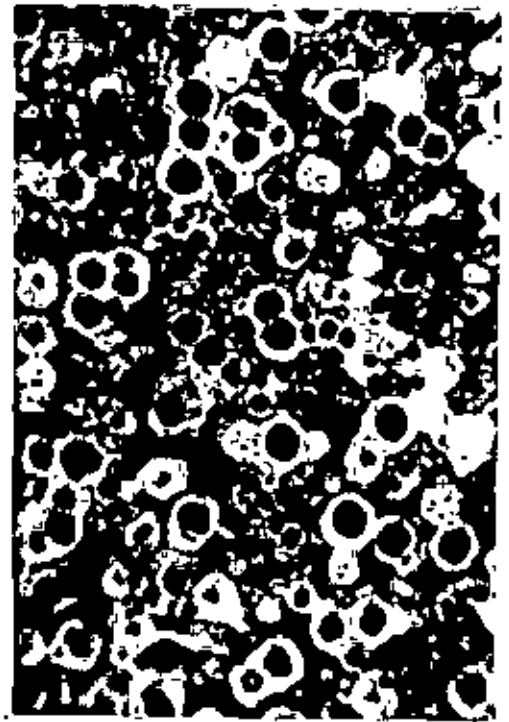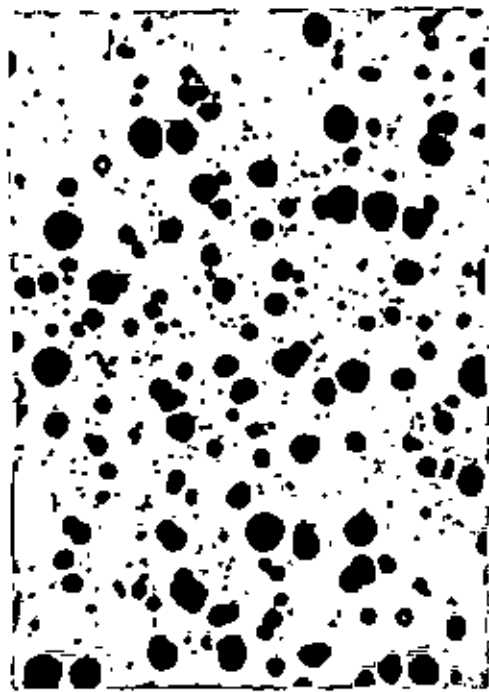
(c)

(d)

Fig 17: Optical micrograph of tensile specimens produced in the 2nd heat.
x100:
- (a) As–Cast tensile specimen B_{11}, unetched
- (b) As–Cast tensile specimen B_{11}, etched
- (c) Annealed (at 950°C for 1 hr.) tensile specimen B_{12} unetched.
- (d) Annealed (at 950°C for 1 hr.) tensile specimen B_{12} etched.
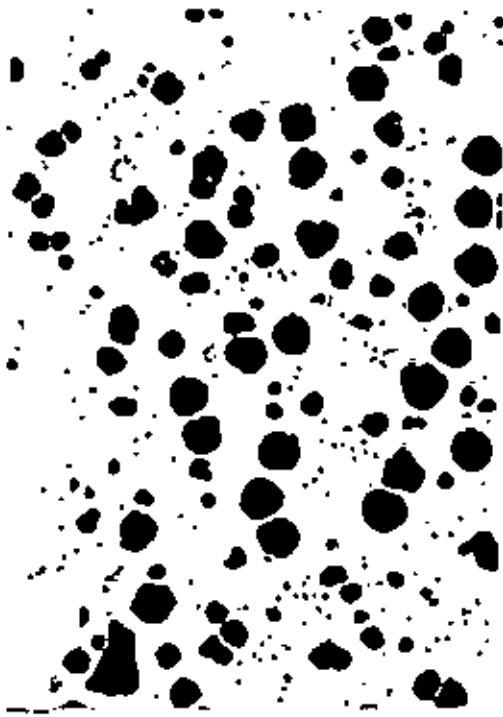
(c)   (d)

Fig 18:   Optical micrograph of tensile specimens produced in the 2nd heat.
x100:
(a)   As–Cast tensile specimen B_{21}, unetched
(b)   As–Cast tensile specimen B_{21}, etched
(c)   Annealed (at 950°C for 1 hr.) tensile specimen B_{22}
unetched.
(d)   Annealed (at 950°C for 1 hr.) tensile specimen B_{22}, etched.

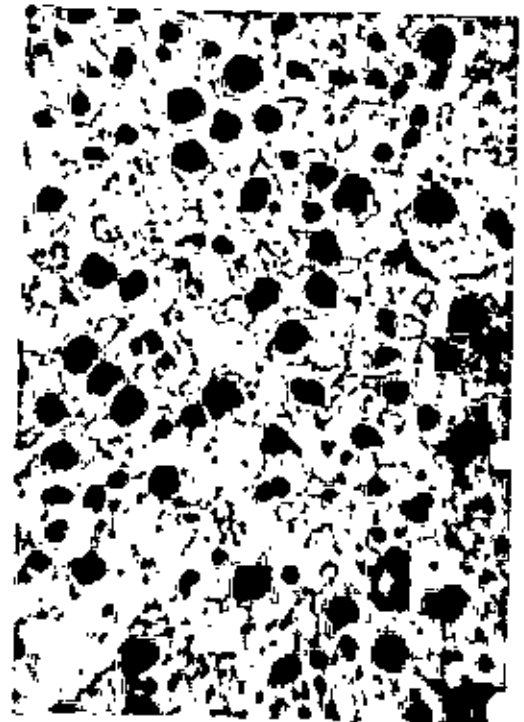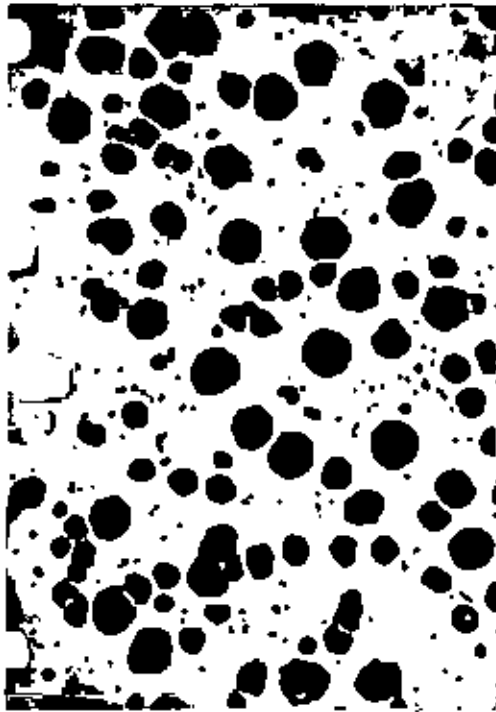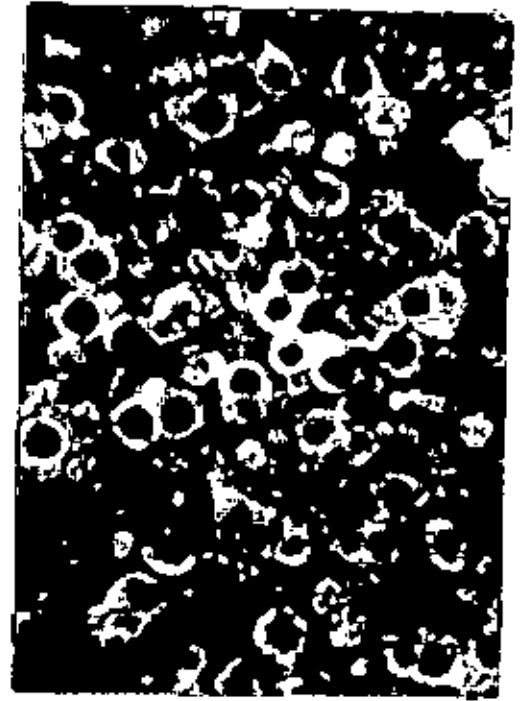In order to observe the mechanical properties and microstructure B_{11} and B_{22} specimens were annealed at 950^0C for 1 hour and then allowed to furnace cool. It was found from the microstructures of unetched annealed tensile specimens (Fig 17c and Fig 18c) that the annealed specimens contained a slightly more number of nodules than those of the as-cast specimens. Due to the annealing treatment, pearlite was dissolved and dispersed in the matrix as a carbon particles. Microstructures of these annealed specimens under etched condition (Fig 17d and Fig 18d) showed ferrite network.

5.3. Mechanical properties of produced S.G. iron

Mechanical properties of specimens cut from the keel block cast in the 1st heat are listed in table-7. Although three numbers of tensile specimens were prepared from the same keel block but slight difference in results were obtained.

Specimen A_1 (table-7) showed lowest U.T.S. but higher percentage of elongation and reduction of area. Whereas specimen A_3 showed the highest U.T.S. with the lowest percentage of elongation and reduction of area amongst the three. Specimen A_2 showed intermediate properties.

The rockwell hardness of these tensile specimens were measured in B scale and it will be found from table-7 that the hardness of these three specimens are more or less same.

It is to be mentioned here that there was a notch on the surface of the tensile specimen A_1. As a result of this notch, the

specimen was fractured under low load.

Specimen A_1 showed better U.T.S. This A3 specimen was cut from the bottom part of the leg of keel block. Due to the rapid solidification of this part compared to the rest of the keel block better nodule sizes and uniform distribution of nodules were observed in the matrix. Less number of ferrite rings were found to form in the matrix of this specimen for this rapid cooling rate. As a result of better nodule size, uniform distribution of nodules and the formation of more pearlite in the matrix the highest strength was obtained in this specimen. Whereas due to the formation of lower number of ferrite rings in the matrix the lowest percentage of elongation and the lowest percentage of reduction in area were obtained. Slower cooling rate allowed longer time for more graphite to develop in the specimen A_1. As a result in the specimen A_1 the largest size of nodules were observed. Due to slow cooling the deterioration of graphite shape was also observed in the microstructure. Larger number of ferrite rings were formed in the specimen A_1 due to slow cooling rate. As a result the lowest U.T.S. and the highest % of elongation and % of reduction in area were obtained. In specimen A_1 intermediate properties were observed because of intermediate cooling rate.

Table-13 shows the mechanical properties of keel block produced in the 2nd heat. In this heat two keel blocks were poured with the same melt. B_1 keel block was poured at first and B_2 later.

In the 2nd heat the highest value of U.T.S., % of elongation and % of reduction in area were observed in the specimens cut from

B_1 keel block comparing to those in the specimens cut from B_2 keel block. Although B_1 and B_2 keel blocks were poured with the same melt, but B_1 keel block was poured at first and B_2 later. Due to the loss of pouring temperature during the pouring of B_2 keel block, lower nodule count, lower nodularity and lower mechanical properties were observed.

Tensile specimens and V-notch impact specimens cut from B_1 and B_2 keel block and denoted as B_{12} and B_{22} respectively were annealed at 950°C for 1 hour. It was found that the strength and the impact energy of these specimens were decreased as a result of annealing treatment. But the percentage of elongation and the percentage of reduction in area were found to increase after annealing treatment. Because the annealing treatment transformed all pearlite into ferrite matrix. As a result of this ferrite structure, the strength and the impact energy were lowered and the ductility was increased.

It is to be mentioned here that the % of elongation and % of reduction in area of the specimen B_{12} could not be measured because it was broken at the outside of the gauge length.

It was found that the castings produced in the 2nd heat showed better mechanical properties than those of castings produced in the 1st heat. High C.E. and post inoculation was responsible for this better mechanical properties of the 2nd heat.

CHAPTER 6

CONCLUSIONS

6.1 <u>Conclusions drawn from the present work</u>

(i) Size of nodules increases with the increase of the thickness of casting bar.

(ii) Nodularity of nodules formed in the bars of thinner sections is better.

(iii) Number of pin like little spheroids increases as the section size increases.

(iv) More carbides are formed as the section thickness decreases.

(v) Formation of ferrite rings are favoured with the increase of section thickness.

(vi) Percentage of ferrite rings increases as the percentage of Si in S.G. iron increases.

(vii) Addition of graphite as a carburizer instead of charcoal increases the C.E. of the melt.

(viii) Higher C.E. and post-inoculation are responsible for better mechanical properties, better nodule count and nodularity and uniform distribution of nodules.

(ix) Annealing treatment transforms the pearlite matrix of tensile specimen of S.G. iron into ferrite matrix.

(x) Annealing treatment lowers U.T.S. but increases the percentage of elongation and the percentage of reduction in area.

(xi) Annealing treatment decomposes the massive carbides in the as-cast thin section bars and allows to disperse as carbon particles in the ferrite matrix resulting more number of nodules in the annealed thin section bars.

6.2 Suggestions for further work

(i) An austempering treatment of S.G. iron should be carried out to observe better mechanical properties. This treatment will result a S.G. iron with exceptionally high in strength and ductility.

(ii) The tensile test of bars of different diameters cast with S.G. iron should be taken to observe the effect of cooling rate on mechanical properties.

(iii) Pig containing lower composition of S, Mn and P should be used as charging material to get better result.

(iv) A study on the elimination of carbide formation in thinner section bars should be carried out. This will help to get larger number of nodules in thinner section bars and to ensure better mechanical properties.

Table 1: <u>Target Composition of S.G. Iron</u>

Composition, wt %			
C	Si	Mg	S
3.30-4.20	1.10-3.50	0.04	0.02 (Max[a])

Table 2: <u>Composition of charge material</u>

Charge material	Composition, wt %						
	C	Si	Mn	P	S	Mg	Fe
Pig iron	3.45	2.80	0.64	0.06	0.12	–	Balance
Mild steel rod	0.30	0.20	0.51	0.04	0.03	–	Balance
Fesi (inoculant)	–	75	–	–	–	–	Balance
FeSiMg	–	42	–	–	–	5.5	Balance

Table 3: <u>Charge for desulphurization in the Ist heat</u>

Charge material	Wt, gm	%C	%Si	%Mn	%P	%S
Pig iron	11,709	3.45	2.80	0.64	0.06	0.12
Mild steel rod	4,140	0.30	0.20	0.51	0.04	0.03
CaC$_2$	75	–	–	–	–	–
Charcoal	151	98	–	–	–	–
Total	16,075	3.51	2.09	–	–	–

Table 4: Composition of desulphurized iron (Ist heat)

Composition, wt %					
C	Si	Mn	P	S	Fe
3.30	2.11	0.68	0.08	0.016	Balance

Table 5: Charge for the production of S.G. iron (Ist heat)

Charge material	Wt, gm	%C	%Si	%Mn	%P	%S	Mg
Desulphurized iron	17,000	3.30	2.11	0.68	0.08	0.016	
FesiMg	272	–	42	–	–	–	5.5
Total	17,272	3.45	2.69				
Inoculant, FeSi (75% Si)	86						

Table 6: Composition of manufactured S.G. iron (Ist heat)

Composition, Wt %						
C	Si	Mn	P	S	Mg	Fe
3.05	2.70	0.60	0.07	0.01	0.05	Balance

Table 7: The effect of the cooling rate on the morphology of graphite, nodule counts, nodularity and matrix of S.G. the iron under as cast and aunealed condition (produced in Ist heat)

Speci-men No.	Section size dia in inch	Morpho-logy of graph-ite (as cast)	Morpho-logy of graph-ite (annea-led)	Nodule count per mm² (as cast)	Nodule count per mm² (annealed)	Nodula-rity (aver-age) as cast)	Nodula-rity (avera-ge) (anne-aled)	Matrix (as cast)	Matrix (annea-led)
1	½	SG +V(Few)	SG +V(Few)	15–50	275–300	90%	92%	P+Cm Cm=45%	Fe
2	¾	SG +V(Few)	SG +V(Few)	50–75	200–225	83%	89%	P+Cm Cm=30%	Fe
3	1	SG+V	SG	75–100	125–130	84%	84%	P+Cm Cm=20%	Fe+P P=4%
4	1½	SG	SG	100–125	100–125	86%	88%	P+Cm+Fe Cm=7% Fe=2%	Fe+P P=6%
5	2	SG	SG	125–130	125–130	83%	89%	P+Fe Fe=4%	Fe+P P=8%
6	2½	SG	SG	130–140	125–130	87%	87%	· P+Fe Fe=8%	Fe+P P=10%

Cm=Cementite, Fe=Ferrite, P=Pearlite, SG=Spheroidal Graphite, V=Vermicular graphite.

Table 8: Mechanical properties along with metallographic data of S.G. iron produced in the Ist heat

Keel block No.	Tensile specimen No.	UTS	% Elon-gation	% Reduc-tion of area	Rock well hardness in B scale	Nodule count per mm²	Nodula-rity	Morphology of graphite	Matrix
A	A₁ (Notch was present)	450 N/mm²	2	7.69	103	125–150	87%	SG+CG(Few)	P+Fe Fe=15%
	A₂	492 N/mm²	1.5	6.31	102	150–175	90%	SG+CG(Few)	P+Fe+Cm Fe=10% Cm=1%
	A₃	562 N/mm²	1	5.52	104	150–175	92%	SG	P+Fe+Cm Fe=10% Cm=1%

Cm= Cementite, Fe=Ferrite, P=Pearlite, SG=Spheroidal Graphite, V=Vermicular graphite.

Table 9: Charge for desulphurisation in the 2nd heat

Charge material	Wt, gm	%C	%Si	%Mn	%P	%S
Pig iron	14,518	3.45	2.80	0.64	0.06	0.12
Mild steel rod	5,134	0.30	0.20	0.51	0.04	0.03
CaC$_2$	160	–	–	–	–	–
Graphite rod	188+38	98	–	–	–	–
Total	20,000	3.51	2.09			

Table 10: Composition of desulphurized iron (2nd heat

Composition, % Wt					
C	Si	Mn	P	S	Fe
3.40	2.14	0.70	0.08	0.01	Balance

Table 11: Charge for the production of S.G. iron (2nd heat)

Charge material	Wt, gm	%C	%Si	%Mn	%P	%S	%Mg
Desulphurized iron	19,682	3.40	2.14	0.70	0.08	0.01	–
FeSiMg	318	–	42	–	–	–	5.5
Total	20,000	3.45	2.69	–	–	–	–
Inoculant, FeSi (75% Si)	100	–	–	–	–	–	–

Table 12: Composition of manufactured S.G. iron (2nd heat)

Composition, % Wt						
C	Si	Mn	P	S	Mg	Fe
3.21	2.73	0.63	0.08	0.01	0.03	Balance

Table 13: Mechanical properties along with metallographic data of S.G.
iron produced in the 2nd heat

Keel block No.	Speci-men No.	Cond-ition	UTS N/mm²	% Elon-gation	% Reduc-tion of area	Rock well hardness in B scale	Impact energy, N mm⁻¹	Nodula-rity	Morpho-logy of graph-ite	Matrix
B₁	B₁₁	As-Cast	667	7	9.27	99	80.75	200-225	SG	Fe+P+Cm Fe=35%, Cm=1%
	B₁₂	Anne-aled	508	23	29	85	75.20	225-250	SG	Fe (100%)
B₂	B₂₁	As-Cast	544	3	3.15	99.30	80.00	175-200	SG	Fe+P+Cm Fe=30%, Cm=1%
	B₂₂	Anne-aled	474	Failed	Failed	85.30	75.50	175-200	SG	Fe (100%)

Cm= Cementite, Fe=Ferrite, P=Pearlite, SG=Spheroidal Graphite.

REFERENCE

1. R. R. Kust and C. R. Loper, 1968, AFS transaction, V-76, P-540-546.

2. Doru M. Stafensen and Dilip K. Bandyopadhyay, 1990, conference proceedings, cast iron IV, 1990, material research society, P-15.

3. J. Kerverian and H. F. Taylor, 1957, AFS Transaction, V-65, P-212.

4. Loper C.R. and R.W. Heine, 1961, AFS Transaction, V-69, P-583.

5. C. R. Kellermann and C. R. Loper, 1965, AFS Transaction, V-72, P-417-425.

6. N. L. Church and R. D. Schelleng, 1970, AFS Transaction, V-78, P 5-8.

7. R. K. Buhr, 1968, AFS Transaction, V-76, P-497-503.

8. C. R. Loper and R. W. Heine, 1965, AFS Transactions V-72, P 495-507.

9. Stephen I. Karsay, Ductile iron production.

10. J. M. Crockett and H. E. Henderson, 1954, AFS Transaction, V-62, P-256-257.

11. I. C. H. Hughes, Oct, 1952, Foundry journal, p-417.

12. H. Gries and V. Maushake, Giesserei, March, 1953, Tech. Wiss. Beih, p-493.

13. E. V. Kovalevich et.al, Aug 1989, Sov. Cast. Technol, Part-8, p-1-3.

14. European pattern application, publication no.EP0347052A$_1$.

15. C. L. Tuggle and R. Carlson, 1970, AFS Transaction, V-78, p-343-349.

16. Trojan P. K. Bargeron, W. N and Flinn, R.A, 1967, AFS Transactions, V75, p-611-624.

17. Dawson, J.V. 1966, AFS Transaction, V-74, p-129-135.

18. W. F. Shaw and T. Watmough, 1969, AFS Transaction, V-77, p-380-386.

19. W. J. Dell and R. J. Christ, 1965, AFS Transaction, V-72, p-408-416.

20. P. K. Basutkar, C. R. Loper and C. L. Babu, 1970, AFS Transaction, V 78, p-432.

21. **Cast Iron Technology, R.Elliott, 1988,Butterworths.**

22. Brandt, F. A. Bishop, H. F. Pellini, W.S. 1950, AFS Transaction, V-62, p-646.

23. Enoukidze Nudor A, Lian Jinjiong, Zhong Weizhen, Rong yu, Nov. 1989, Jour of univ. of Sc. and Tech, Beijing, V-8, p-545.